A strain-displacement mixed formulation based on the modified couple stress theory for the flexural behaviour of laminated beams.

Luan C. Trinh [a,*], Rainer M.J. Groh [b], Giovanni Zucco [a], Paul M. Weaver [a, b]

[a] Bernal Institute, School of Engineering, University of Limerick, Castletroy, V94 T9PX, Ireland

[b] Bristol Composites Institute (ACCIS), Department of Aerospace Engineering, University of Bristol, Queen's Building, University Walk, Bristol BS8 1TR, UK

Abstract

A novel strain-displacement variational formulation for the flexural behaviour of laminated composite beams is presented, which accurately predicts three-dimensional stresses, yet is computationally more efficient than 3D finite element models. A global third-order and layer-wise zigzag profile is assumed for the axial deformation field through the laminate thickness to account for the effect of both stress-channelling and stress localisation. By using this axiomatic kinematic field, a variational formulation is developed based on an equivalent single layer theory such that the number of unknowns is independent of the number of composite layers. The axial and couple stresses are evaluated from the displacement field, while the transverse shear and transverse normal stresses are computed by the interlaminar-continuous equilibrium conditions within the framework of the modified couple stress theory. Axial and transverse force equilibrium conditions are imposed via two Lagrange multipliers, which correspond to the axial and transverse displacements. Using this mixed variational approach, both displacements and strains are treated as unknown quantities, resulting in more functional freedom to minimise the total strain energy. In this work, two strain-displacement-based models are developed to investigate the effect of couple stress on the flexural behaviour of composite beams. The first model neglects the presence of couple stress, whilst the second includes couple stress with an additional unknown curvature. The differential quadrature method is used to solve the resulting governing and boundary equations for simply-supported and clamped laminated beams. For the simply-supported case, numerical results from this variational formulation for both models agree well with those from a Hellinger-Reissner stress-displacement mixed model found in the literature and the 3D elasticity solution given by Pagano. For the clamped laminate, the additional curvature associated with the couple stress plays an important role in accurately predicting stresses, which is confirmed by a high-fidelity 3D finite element model.

Keywords: Strain-displacement mixed formulation; modified couple stress; laminated beam; stress analysis; zigzag theory.

* Corresponding author. E-mail address: luan.trinh@ul.ie (Luan C. Trinh)

Nomenclature

x, z = longitudinal and transverse coordinates of the beam

$(\bullet)_{,x}$ or $(\bullet)_{,z}$ = derivative of $(\bullet)$ with respect to x or z

t = thickness of the beam

$t^{(k)}$ = thickness of kth lamina

z_{k-1}, z_k = lower and upper coordinate of kth lamina

$\mathcal{F}_s = \begin{bmatrix} N & M & O & P & L \end{bmatrix}^T$ = vectors of stress resultants

u_0 = in-plane displacement of neutral axis in x-direction

θ = rotation of cross-section

ζ, ξ = higher-order rotations of cross-section

ψ = zigzag displacement

w_0 = transverse displacement

$\mathcal{U} = \begin{bmatrix} u_0 & \theta & \psi & \zeta & \xi \end{bmatrix}^T$ = vector of displacement components

$\boldsymbol{\chi}_{xy}$ = $\begin{bmatrix} u_{0,x} & \theta_{,x} & \psi_{,x} & \zeta_{,x} & \xi_{,x} & w_{0,xx} \end{bmatrix}^T$

$\boldsymbol{\chi}_{zy}$ = $\begin{bmatrix} \zeta & \xi \end{bmatrix}^T$

$\sigma_x^{(k)}, \tau_{xz}^{(k)}, \sigma_z^{(k)}$ = longitudinal, transverse shear and transverse normal stresses

$\varepsilon_x^{(k)}, \gamma_{xz}^{(k)}, \varepsilon_z^{(k)}$ = longitudinal, transverse shear and transverse normal strains

$\overline{Q}_{11}^{(k)}$ = transformed axial stiffness matrix for kth lamina

$G_{xz}^{(k)}(x)$ = transformed transverse stiffness matrix for kth lamina

$\theta_x^{(k)}, \theta_y^{(k)}, \theta_z^{(k)}$ = micro-rotation about x, y and z axes

$m_{xy}^{(k)}, m_{zy}^{(k)}$ = couple-stresses exerted on x- and z-surfaces, respectively, and bending these surfaces about the y-axis

$\tilde{Q}_{44}^{(k)}, \tilde{Q}_{66}^{(k)}$ = transformed couple-stress stiffness matrix for kth lamina

λ_1, λ_2 = Lagrange multipliers

1. Introduction

Laminated structures have been increasingly applied in many engineering sectors such as aerospace, automotive, naval and sports thanks to their extraordinary strength- and stiffness-to-weight ratios. It is also widely appreciated that these materials present anisotropic responses, for example, axial stress-channelling and significant through-thickness transverse shear stress in bending. Therefore, developing an advanced model to capture such behaviours accurately and efficiently is one of the main streams in computational mechanics. From the application point of view, the displacement-based axiomatic models have been widely used for analysing the main components of laminated structures due to their computational effectiveness. One of the earliest axiomatic models for analysing laminated beams is rooted in classical beam theory (CBT) [1], which assumes that the cross-section remains undistorted and perpendicular to the beam axis. Later, first-order shear deformation beam theory (FBT) [2] was developed neglecting the second assumption in the CBT by adding cross-sectional rotation as a variable. However, these theories are rarely implemented in the stress analysis of laminated structures as they cannot capture in-plane and transverse stresses and strains of highly heterogeneous laminates [3] with sufficient accuracy. Rather, they are used as a starting point to develop higher-order theories and equivalent single layer zigzag (ZZ) models [4-16] or in analysing the vibration and buckling behaviours of such structures [17-19]. They are also employed to develop couple-stress based models, which can be used to predict the size effect from sub-scale components, *i.e.* the interaction of fibres or voids within laminae, to the upper scales by using the gradients of displacement as micro-rotations [20-25]. To improve the accuracy of the equivalent single-layer (ESL) models, a unified formulation (UF) was proposed by Carrera and co-authors [26], which is based on a hierarchical structure that can recover CBT, FBT and higher-order beam theories. This model has been applied extensively to many beam problems [12, 27-33]. Another type of higher-order ESL models, that can capture both axial stress channelling and the stress-free condition of shear stresses at the surfaces, are the higher-order shear deformation theories (HSDT), which were developed by assuming a higher-order polynomial, trigonometric or exponential axial displacement. Some interesting publications regarding the HSDTs can be found in [13, 14, 34-38]. These HSDT models are in general not as accurate as UF models but require much less computational cost. It is worth mentioning that the displacement in the HSDTs are continuous through-thickness, resulting in a continuous shear strain, hence violating the continuity condition of shear stresses between layers of different in-plane shear moduli. One possible remedy is to use the through-thickness zigzag displacement field, which initiates discontinuous layer-wise shear strains and allows the shear stresses to satisfy the interlaminar continuity condition. From the historical review conducted by Carrera [39], ZZ theories can be divided into three groups according to models by Lekhnitskii, Ambartsumian and Reissner. Later, Tessler *et al.* [9, 40] refined ZZ theory by accounting for the difference between laminae shear rigidities and the effective shear rigidity of the laminate. This refined zigzag theory (RZT), especially when combined with the higher-order global displacement [41], has shown excellent agreement with Pagano's exact solutions. Also, many recent publications have shown successful applications of RZT for various behaviours of beams and plates [6, 7, 42-50].

In recent years, multi-scale analysis has become an appealing strategy to reduce the computational expense in modelling multi-scale structures. One of the approaches which has been widely applied in multi-scale analysis is the higher-order continuum, in which the additional micro-rotations at material point is included in the kinematic description to transfer the effect from sub-scale constituents to the considered structure, for example, the effect from fibre rotation to lamina behaviour in a homogenised lamina. Various approaches have been proposed for the calculation of the micro-rotation resulting in micro-continua including the micropolar, microstretch and micromorphic by Eringen [51-54] and the strain gradient theories by Mindlin [55-58]. Within the framework of strain gradient theories, Yang et al. [59, 60] introduced an additional moment equilibrium leading to the symmetry of couple stress results and reduction of the number of material constants, *i.e.* the length scales, in the constitutive relation for isotropic materials. Chen et al. [61, 62] recently modified the constitutive law in the modified couple stress theory to investigate the orthotropy in material length scales for laminated structures. To the best of the authors' knowledge, these theories have not yet been developed for investigating the effects of laminae interactions to the laminate level.

Apart from enriching kinematics fields, the mixed variational formulation is another approach for improving the accuracy in structural analysis of laminated composites by giving more freedom to the functional unknowns. Many mixed formulations have been proposed from the Hu-Washizu (HW) principle [63] to the Hellinger-Reissner (HR) principle [64] and the Reissner mixed variational theory (RMVT) [65]. The HW principle can be considered as the most general principle, in fact it allows the independence of all three displacement, strain and stress variables. As discussed by Militello and Felippa in [66], the HR can be deduced from the HW principle by equating the strain from the kinematics and the strains from the stress assumption. Similarly, the RVMT can be obtained by eliminating the stress independence. Due to their efficiency in predicting the structural response of composite structures, many publications can be found employing the HR principle [67-72] and the RVMT principle [7, 47, 48, 73, 74]. Recently, Groh and Weaver [41] performed a comparison of these two mixed formulations in the stress analysis of laminated and sandwich beams using the axiomatic third-order zigzag displacement field though-the-thickness and concluded that both formulations provide matching axial stress results with the 3D exact solution given by Pagano, but the RVMT principle requires a post-processing step to obtain transverse stress.

The present study aims to develop a novel strain-displacement (SD) mixed formulation in which the functional freedom is given for the generalised strains and displacements while the through-thickness strains and stresses are calculated from the third-order zigzag displacements, which have been proposed by Groh and Weaver [41] within the framework of the Hellinger-Reissner principle and denoted by HR3-RZT in this paper. Furthermore, this SD mixed formulation is developed within the modified couple stress (MCS) theory to form a SD MCS solution.

The proposed strain-displacement formulations, *i.e.* SD and SD MCS, are firstly validated for simply-supported beams in Section 3.1. These formulations are further applied to a non-symmetric clamped beam and validated against a 3D solution modelled in Abaqus [75] in Section 3.2. Finally, in Section 4 conclusions are drawn.

2. Mathematical formulation

Consider a laminated beam, as shown in Fig. 1, with length and rectangular cross-section L and $b \times t$, respectively. The term b indicates the width of the beam, while t the thickness of the laminate. The beam has N layers and the materials in each layer can be different. The beam is associated with the Cartesian coordinate system (x, y, z) where x is the longitudinal axis, z the thickness and y the width directions. The fibres are in the x-y plane and the fibre orientation $\theta^{(k)}$ in k^{th} layer is referred to the x-axis. The beam is loaded with shear tractions $\hat{T}_t$ and $\hat{T}_b$, and normal tractions $\hat{P}_t$ and $\hat{P}_b$ at the top and bottom, respectively.

2.1. Higher-order zigzag displacement theory

In the third-order refined zigzag theory, the longitudinal and transverse displacements are assumed as follows

$$u_x^{(k)}(x,z) = u_0 + z\theta + z^2\zeta + z^3\xi + \phi^{(k)}(z)\psi\,, \tag{1a}$$

$$u_z(x) = w_0\,, \tag{1b}$$

where $\mathbf{f}_{\phi_u}^{(k)}(z) = \begin{bmatrix} 1 & z & z^2 & z^3 & \phi^{(k)}(z) \end{bmatrix}$ is the shape function to define the thickness-wise profile of the pertinent displacement components $\boldsymbol{\mathcal{U}}$. The refined zigzag function $\phi^{(k)}(z)$ is defined for the first layer and the kth layer as follows [9, 41]

$$\phi^{(1)}(z) = \left(z + \frac{t}{2}\right)\left(\frac{G}{G_{xz}^{(1)}} - 1\right), \tag{2a}$$

$$\phi^{(k)}(z) = \left(z + \frac{t}{2}\right)\left(\frac{G}{G_{xz}^{(k)}} - 1\right) + \sum_{j=2}^{k} t^{(j-1)}\left(\frac{G}{G_{xz}^{(j-1)}} - \frac{G}{G_{xz}^{(k)}}\right), \tag{2b}$$

where $G_{xz}^{(k)}$ and $G = \left[\frac{1}{t}\sum_{k=1}^{N}\frac{t^{(k)}}{G_{xz}^{(k)}}\right]^{-1}$ are the shear modulus of each layer and equivalent shear modulus of the laminate, respectively. The layerwise zigzag function in Eq. (2) can be rewritten as $\phi^{(k)}(z) = g_{ZZF}^{(k)} z + c_{ZZF}^{(k)}$, where $g_{ZZF}^{(k)}$ and $c_{ZZF}^{(k)}$ are the linear and constant terms, respectively.

The axial strain corresponding to the kinematics of Eq. (1) is measured by

$$\varepsilon_x^{(k)} = \frac{\partial u_x}{\partial x} = \mathbf{f}_{\phi_u}^{(k)}\boldsymbol{\mathcal{U}}_{,x} = \mathbf{f}_{\phi_u}^{(k)}\boldsymbol{\varepsilon}\,, \tag{3}$$

where $\boldsymbol{\varepsilon} = \boldsymbol{\mathcal{U}}_{,x}$ is an equivalent strain vector of stretching, curvature, and higher-order curvature terms on the reference plane, and the comma notation denotes differentiation.

Using the constitutive law, the axial stress is expressed through the strain vector as

$$\sigma_x^{(k)} = \overline{Q}_{11}^{(k)}\varepsilon_x^{(k)} = \overline{Q}_{11}^{(k)}\mathbf{f}_{\phi_u}^{(k)}\boldsymbol{\varepsilon}\,. \tag{4}$$

Therefore, the stress resultants are defined from the displacement field of Eq. (1) as follows

$$\boldsymbol{\mathcal{F}} = \int_{-t/2}^{t/2} \mathbf{f}_{\phi_u}^{(k)^T} \sigma_x^{(k)} dz = \int_{-t/2}^{t/2} \mathbf{f}_{\phi_u}^{(k)^T} \overline{Q}_{11}^{(k)} \mathbf{f}_{\phi_u}^{(k)} dz \boldsymbol{\varepsilon} = \mathbf{S}\boldsymbol{\varepsilon}\,, \tag{5}$$

where the constitutive stiffness matrix $\mathbf{S}$ is defined in according to [41] as

$$\mathbf{S} = \begin{bmatrix} A & B & D & E & B_\phi \\ B & D & E & F & D_\phi \\ D & E & F & H & E_\phi \\ E & F & H & I & F_\phi \\ B_\phi & D_\phi & E_\phi & F_\phi & D_{\phi\phi} \end{bmatrix}, \tag{6}$$

and the beam stiffness constants are evaluated by the following integrals,

$$\left(A, B, D, E, F, H, I\right) = \sum_{k=1}^{N} \int_{z_k}^{z_{k+1}} \overline{Q}_{11}^{(k)} \left(1, z, z^2, z^3, z^4, z^5, z^6\right) dz\,, \tag{7a}$$

$$\left(B_\phi, D_\phi, E_\phi, F_\phi, D_{\phi\phi}\right) = \sum_{k=1}^{N} \int_{z_k}^{z_{k+1}} \overline{Q}_{11}^{(k)} \phi^{(k)} \left(1, z, z^2, z^3, \phi^{(k)}\right) dz\,. \tag{7b}$$

To be compatible with the vector of curvature in the couple stresses, Eq. (5) is rewritten by adding $w_{0,xx}$ corresponding to the micro-curvature to the strain vector as below,

$$\boldsymbol{\mathcal{F}}_s = \mathbf{S}_s \boldsymbol{\chi}_{xy}\,, \tag{8a}$$

where $\boldsymbol{\mathcal{F}}_s = \begin{Bmatrix} \boldsymbol{\mathcal{F}} \\ 0 \end{Bmatrix}$; $\mathbf{S}_s = \begin{bmatrix} \mathbf{S} & \mathbf{0} \\ \mathbf{0} & 0 \end{bmatrix}$; and $\boldsymbol{\chi}_{xy} = \begin{Bmatrix} \boldsymbol{\varepsilon} \\ w_{0,xx} \end{Bmatrix}$. (8b)

In the present work, the equilibrium conditions and strain energy are computed within the framework of the modified couple stress theory [76]. In this couple stress theory, the additional degrees of freedom, *i.e.* micro-rotations, are calculated by the *curl* of displacements, and the pertinent micro-curvatures are measured from the gradient of these micro-rotations. The micro-curvatures are energetically conjugate to the couple stresses, which are used to determine the strain energy by couple stresses.

The micro-rotations and corresponding micro-curvatures are calculated from the displacements as follows

$$\boldsymbol{\theta} = \frac{1}{2} curl\, \mathbf{u} = \frac{1}{2}\left[\left(\mathrm{u}_{z,y} - \mathrm{u}_{y,z}\right)\mathbf{e}_\mathbf{x} + \left(\mathrm{u}_{x,z} - \mathrm{u}_{z,x}\right)\mathbf{e}_\mathbf{y} + \left(\mathrm{u}_{y,x} - \mathrm{u}_{x,y}\right)\mathbf{e}_\mathbf{z}\right], \tag{9a}$$

$$\boldsymbol{\chi} = \left[\nabla\boldsymbol{\theta} + \left(\nabla\boldsymbol{\theta}\right)^T\right]. \tag{9b}$$

For beams being deformed in the *x*-*z* plane, the non-zero micro-rotations and micro-curvatures are

$$\theta_y^{(k)} = \frac{1}{2}\left(\mathbf{f}_{\phi_u,z}^{(k)} \boldsymbol{\mathcal{U}} - w_{0,x}\right), \tag{10a}$$

$$\chi_{xy}^{(k)} = \frac{1}{2}\mathbf{f}_{c_1}^{(k)} \boldsymbol{\chi}_{xy}\,,\ \chi_{zy}^{(k)} = \frac{1}{2}\mathbf{f}_{c_2}^{(k)} \boldsymbol{\chi}_{zy}\,, \tag{10b}$$

where the shape functions determining the contribution of couple stresses through thickness are addressed by

$$\mathbf{f}_{c_1}^{(k)}=\begin{bmatrix}0 & 1 & 2z & 3z^2 & \phi_{,z}^{(k)} & -1\end{bmatrix},\ \boldsymbol{\chi}_{xy}=\begin{bmatrix}u_{0,x} & \theta_{,x} & \psi_{,x} & \zeta_{,x} & \xi_{,x} & w_{0,xx}\end{bmatrix}^T, \tag{11a}$$

$$\mathbf{f}_{c_2}^{(k)}=\begin{bmatrix}2 & 6z\end{bmatrix},\ \boldsymbol{\chi}_{zy}=\begin{bmatrix}\zeta & \xi\end{bmatrix}^T. \tag{11b}$$

The couple stresses are expressed through the curvatures as follows

$$m_{xy}^{(k)}=\tilde{Q}_{44}^{(k)}\chi_{xy}^{(k)}=\frac{1}{2}\tilde{Q}_{44}^{(k)}\mathbf{f}_{c_1}^{(k)}\boldsymbol{\chi}_{xy}, \tag{12a}$$

$$m_{zy}^{(k)}=\tilde{Q}_{66}^{(k)}\chi_{zy}^{(k)}=\frac{1}{2}\tilde{Q}_{66}^{(k)}\mathbf{f}_{c_2}^{(k)}\boldsymbol{\chi}_{zy}, \tag{12b}$$

where $\tilde{Q}_{44}^{(k)}$ and $\tilde{Q}_{66}^{(k)}$ are the additional constitutive constants corresponding to the spanwise and thickness wise length scales, which are defined by [77]

$$\tilde{Q}_{44}^{(k)}=l_{kb}^2G_{13}^{(k)}m^2\left(m^2-n^2\right)-l_{km_1}^2G_{23}^{(k)}n^2\left(m^2-n^2\right)+2m^2n^2\left(l_{kb}^2G_{13}^{(k)}+l_{km_1}^2G_{23}^{(k)}\right), \tag{13a}$$

$$\tilde{Q}_{66}^{(k)}=l_{km_2}^2\left(G_{23}^{(k)}m^2+G_{13}^{(k)}n^2\right), \tag{13b}$$

where l_{kb}^2, $l_{km_1}^2$ and $l_{km_2}^2$ are the length scale parameters, in which $l_{km_1}^2$ and $l_{km_2}^2$ are small compared to l_{kb}^2 [77, 78] such that $m_{zy}^{(k)}$ is negligible.

2.2. Equilibrium of the equivalent single layer beam based on the modified couple stress theory

The equilibrium equations developed from the variational principle for the modified couple stress theory [76] is written for the beam deforming in x-z plane as follows

$$\sigma_{x,x}^{(k)}+\tau_{xz,z}^{(k)}-\frac{1}{2}\left(m_{xy,xz}^{(k)}+m_{zy,zz}^{(k)}\right)=0, \tag{14a}$$

$$\tau_{xz,x}^{(k)}+\sigma_{z,z}^{(k)}+\frac{1}{2}\left(m_{xy,xx}^{(k)}+m_{zy,xz}^{(k)}\right)=0. \tag{14b}$$

Integrating Eq. (14a) through the z-direction, the axial force equilibrium is obtained

$$\begin{aligned}0&=\int_{z_0}^{z_N}\left[\sigma_{x,x}^{(k)}+\tau_{xz,z}^{(k)}-\frac{1}{2}\left(m_{xy,xz}^{(k)}+m_{zy,zz}^{(k)}\right)\right]dz\\&=N_{,x}+\tau_{xz,z}^{(k)}\Big|_{z_0}^{z_N}-\frac{1}{2}m_{xy,x}^{(k)}\Big|_{z_0}^{z_N}-\frac{1}{2}m_{zy,z}^{(k)}\Big|_{z_0}^{z_N}.\end{aligned} \tag{15}$$

The moment equilibrium is derived after multiplying Eq. (14a) by z and integrating the resulting equation though the thickness

$$\begin{aligned}0&=\int_{z_0}^{z_N}z\left[\sigma_{x,x}^{(k)}+\tau_{xz,z}^{(k)}-\frac{1}{2}\left(m_{xy,xz}^{(k)}+m_{zy,zz}^{(k)}\right)\right]dz\\&=M_{,x}+\left(z\tau_{xz}^{(k)}\Big|_{z_0}^{z_N}-\int_{z_0}^{z_N}\tau_{xz}^{(k)}dz\right)-\frac{1}{2}\left(zm_{xy,x}^{(k)}\Big|_{z_0}^{z_N}-\int_{z_0}^{z_N}m_{xy,x}^{(k)}dz\right)-\frac{1}{2}\left(zm_{zy,z}^{(k)}\Big|_{z_0}^{z_N}-m_{zy,z}^{(k)}\Big|_{z_0}^{z_N}\right).\end{aligned} \tag{16}$$

By noting that $Q=\int_{z_0}^{z_N}\tau_{xz}^{(k)}dz$, the shear force can be expressed in terms of moment, shear stress and couple stresses as follows

$$Q = M_{,x} + z\tau_{xz}^{(k)}\Big|_{z_0}^{z_N} - \frac{1}{2}\left(zm_{xy,x}^{(k)}\Big|_{z_0}^{z_N} - \int_{z_0}^{z_N} m_{xy,x}^{(k)} dz \right) - \frac{1}{2}\left(zm_{zy,z}^{(k)}\Big|_{z_0}^{z_N} - m_{zy,z}^{(k)}\Big|_{z_0}^{z_N} \right). \tag{17}$$

Similarly, integrating (14b) through thickness gives the transverse equilibrium

$$\int_{z_0}^{z_N} \tau_{xz,x}^{(k)} + \sigma_{z,z}^{(k)} + \frac{1}{2}\left(m_{xy,xx}^{(k)} + m_{zy,xz}^{(k)} \right) dz = 0 \tag{18a}$$

$$\therefore Q_{,x} + \left(\hat{P}_t - \hat{P}_b \right) + \frac{1}{2}\int_{z_0}^{z_N} m_{xy,xx}^{(k)} dz + \frac{1}{2} m_{zy,x}^{(k)}\Big|_{z_0}^{z_N} = 0 \tag{18b}$$

Substituting Q from Eq. (17) to Eq. (18b), the new transverse force equilibrium is obtained

$$M_{,xx} + \int_{z_0}^{z_N} m_{xy,xx}^{(k)} dz + z\left(\hat{T}_{t,x} - \hat{T}_{b,x} \right) + \left(\hat{P}_t - \hat{P}_b \right)$$

$$-\frac{1}{2} zm_{xy,xx}^{(k)}\Big|_{z_0}^{z_N} - \frac{1}{2}\left(zm_{zy,zx}^{(k)}\Big|_{z_0}^{z_N} - m_{zy,zx}^{(k)}\Big|_{z_0}^{z_N} \right) + \frac{1}{2} m_{zy,x}^{(k)}\Big|_{z_0}^{z_N} = 0 . \tag{19}$$

Neglecting the external couple-stresses and noting that $\tau_{xz}^{(N)}\left(z_N \right) = \hat{T}_t$; $\tau_{xz}^{(0)}\left(z_0 \right) = \hat{T}_b$; $\sigma_z^{(N)}\left(z_N \right) = \hat{P}_t$; and $\sigma_z^{(0)}\left(z_0 \right) = \hat{P}_b$, Eq. (19) is simplified further as follows

$$M_{,xx} + \int_{z_0}^{z_N} m_{xy,xx}^{(k)} dz + z\left(\hat{T}_{t,x} - \hat{T}_{b,x} \right) + \left(\hat{P}_t - \hat{P}_b \right) = 0 . \tag{20}$$

2.3. Derivation of transverse shear and normal stresses

The shear stress $\tau_{xz}^{(k)}$ is calculated from equilibrium equation (14a)

$$\tau_{xz}^{(k)} = -\int \left[\frac{d\sigma_x^{(k)}}{dx} - \frac{1}{2}\left(\frac{\partial^2 m_{xy}^{(k)}}{\partial x \partial z} + \frac{\partial^2 m_{zy}^{(k)}}{\partial z^2} \right) \right] dz$$

$$= \left(-\bar{Q}_{11}^{(k)} \mathbf{g}_{\phi}^{(k)} + \frac{1}{4}\tilde{Q}_{44}^{(k)} \mathbf{f}_{c_1}^{(k)} \right) \boldsymbol{\chi}_{xy,x} + \mathbf{a}^{(k)}, \tag{21}$$

where

$$\mathbf{g}_{\phi}^{(k)} = \left[z \quad \frac{z^2}{2} \quad \frac{z^3}{3} \quad \frac{z^4}{4} \quad g_{ZZF}^{(k)} \frac{z^2}{2} + c_{ZZF}^{(k)} z \quad 0 \right]. \tag{22}$$

The constant vector $\mathbf{a}^{(k)}$ is obtained by enforcing the interlaminar conditions as presented in Appendix 1 and summarised below

$$\mathbf{a}^{(k)} = \boldsymbol{\alpha}_{c_1}^{(k)} \boldsymbol{\chi}_{xy,x} + \hat{T}_b , \tag{23}$$

where

$$\boldsymbol{\alpha}_{c_1}^{(k)} = \sum_{i=1}^{k} \left[\bar{Q}_{11}^{(i)} \mathbf{g}_{\phi}^{(i)}\left(z_{i-1} \right) - \bar{Q}_{11}^{(i-1)} \mathbf{g}_{\phi}^{(i-1)}\left(z_{i-1} \right) \right] - \frac{1}{4}\sum_{i=1}^{k} \left[\tilde{Q}_{44}^{(i)} \mathbf{f}_{c_1}^{(i)}\left(z_{i-1} \right) - \tilde{Q}_{44}^{(i-1)} \mathbf{f}_{c_1}^{(i-1)}\left(z_{i-1} \right) \right]. \tag{24}$$

The shear stress is expressed compactly in terms of the equivalent strain as follows

$$\tau_{xz}^{(k)} = \mathbf{c}_{c_1}^{(k)} \boldsymbol{\chi}_{xy,x} + \hat{T}_b , \tag{25}$$

where

$$\mathbf{c}_{c_1}^{(k)} = -\bar{Q}_{11}^{(k)}\mathbf{g}_{\phi}^{(k)} + \frac{1}{4}\tilde{Q}_{44}^{(k)}\mathbf{f}_{c_1}^{(k)} + \boldsymbol{\alpha}_{c_1}^{(k)}. \tag{26}$$

Similarly, the normal transverse stress is calculated from equilibrium equation as follows

$$\sigma_z^{(k)} = -\int\left[\frac{d\tau_{xz}^{(k)}}{dx} + \frac{1}{2}\left(\frac{\partial^2 m_{xy}^{(k)}}{\partial x^2} + \frac{\partial^2 m_{zy}^{(k)}}{\partial x \partial z}\right)\right]dz$$

$$= \left(\bar{Q}_{11}^{(k)}\mathbf{h}_{\phi}^{(k)} - \frac{1}{4}\tilde{Q}_{44}^{(k)}\mathbf{g}_{c_1}^{(k)} - \boldsymbol{\alpha}_{c_1}^{(k)}z\right)\boldsymbol{\chi}_{xy,xx} - \frac{1}{4}\tilde{Q}_{44}^{(k)}\mathbf{g}_{c_1}^{(k)}\boldsymbol{\chi}_{xy,xx} - \hat{T}_{b,x}z + \mathbf{b}^{(k)}$$

$$= \left(\bar{Q}_{11}^{(k)}\mathbf{h}_{\phi}^{(k)} - \frac{1}{2}\tilde{Q}_{44}^{(k)}\mathbf{g}_{c_1}^{(k)} - \boldsymbol{\alpha}_{c_1}^{(k)}z\right)\boldsymbol{\chi}_{xy,xx} - \hat{T}_{b,x}z + \mathbf{b}^{(k)}, \tag{27}$$

where

$$\mathbf{h}_{\phi}^{(k)} = \left[\frac{z^2}{2} \quad \frac{z^3}{6} \quad \frac{z^4}{12} \quad \frac{z^5}{20} \quad g_{ZZF}^{(k)}\frac{z^3}{6} + c_{ZZF}^{(k)}\frac{z^2}{2} \quad 0\right], \tag{28a}$$

$$\mathbf{g}_{c_1}^{(k)} = \left[0 \quad z \quad z^2 \quad z^3 \quad \phi_{,z}^{(k)}z \quad -z\right]. \tag{28b}$$

By enforcing the continuity of the transverse normal stress through laminae detailed in Appendix 2, the generic constant at kth layer is presented as follows

$$\mathbf{b}^{(k)} = \boldsymbol{\beta}_{c_1}^{(k)}\boldsymbol{\chi}_{xy,xx} + \hat{T}_{b,x}z_0 + \hat{P}_b, \tag{29}$$

where

$$\boldsymbol{\beta}_{c_1}^{(k)} = -\sum_{i=1}^{k}\left[\bar{Q}_{11}^{(i)}\mathbf{h}_{\phi}^{(i)}(z_{i-1}) - \bar{Q}_{11}^{(i-1)}\mathbf{h}_{\phi}^{(i-1)}(z_{i-1})\right]$$

$$+\sum_{i=1}^{k}\left\{\frac{1}{2}\left[\tilde{Q}_{44}^{(i)}\mathbf{g}_{c_1}^{(i)}(z_{i-1}) - \tilde{Q}_{44}^{(i-1)}\mathbf{g}_{c_1}^{(i-1)}(z_{i-1})\right] + \left(\boldsymbol{\alpha}_{c_1}^{(i)} - \boldsymbol{\alpha}_{c_1}^{(i-1)}\right)z_{i-1}\right\}, \tag{30}$$

Finally, the transverse normal stress is expressed in the compact form of the equivalent strain

$$\sigma_z^{(k)} = \left(\bar{Q}_{11}^{(k)}\mathbf{h}_{\phi}^{(k)} - \frac{1}{2}\tilde{Q}_{44}^{(k)}\mathbf{g}_{c_1}^{(k)} - \boldsymbol{\alpha}_{c_1}^{(k)}z + \boldsymbol{\beta}_{c_1}^{(k)}\right)\boldsymbol{\chi}_{xy,xx} + \hat{T}_{b,x}z_0 + \hat{P}_b$$

$$= \mathbf{e}_{c_1}^{(k)}\boldsymbol{\chi}_{xy,xx} - \hat{T}_{b,x}(z - z_0) + \hat{P}_b, \tag{31}$$

where

$$\mathbf{e}_{c_1}^{(k)} = \bar{Q}_{11}^{(k)}\mathbf{h}_{\phi}^{(k)} - \left[\frac{1}{2}\tilde{Q}_{44}^{(k)}\mathbf{g}_{c_1}^{(k)}(z) + \boldsymbol{\alpha}_{c_1}^{(k)}z\right] + \boldsymbol{\beta}_{c_1}^{(k)}. \tag{32}$$

2.4. Strain-displacement variational formulation for laminated beams

The transverse shear strain is defined by using the constitutive equation

$$\gamma_{xz}^{(k)} = \frac{\tau_{xz}^{(k)}}{G_{xz}^{(k)}} = \frac{1}{G_{xz}^{(k)}}\left(\mathbf{c}_{c_1}^{(k)}\boldsymbol{\chi}_{xy,x} + \hat{T}_b\right). \tag{33}$$

Similarly, the transverse normal strain $\varepsilon_z^{(k)}$ is derived from the plane strain state in the *y*-direction using the full compliance matrix

$$\begin{aligned}\varepsilon_z^{(k)} &= R_{13}^{(k)}\sigma_x^{(k)} + R_{33}^{(k)}\sigma_z^{(k)} \\ &= R_{13}^{(k)}\overline{Q}^{(k)}\mathbf{f}_{\phi}^{(k)}\boldsymbol{\chi}_{xy} + R_{33}^{(k)}\left[\mathbf{e}_{c_1}^{(k)}\boldsymbol{\chi}_{xy,xx} - \hat{T}_{b,x}\left(z - z_0\right) + \hat{P}_b\right],\end{aligned} \tag{34}$$

where $R_{ij} = S_{ij} - \dfrac{S_{i2}S_{j2}}{S_{22}}$, and S_{ij} is the full compliance matrix [41].

Following the Lagrange multipliers approach given in [41], the first variation of the potential energy functional including potentials of the Lagrange multipliers is set to be zero to achieve the equilibrium of system, such that,

$$0 = \delta\Pi = \delta\Pi_{\sigma_x} + \delta\Pi_c + \delta\Pi_{\tau_{xz}} + \delta\Pi_{\sigma_z} + \delta\Pi_{\Gamma} + \delta\Pi_{\lambda}, \tag{35}$$

in which, the variations of potentials of axial stress Π_{σ_x}, couple stress Π_c, transverse shear stress $\Pi_{\tau_{xz}}$, transverse normal stress Π_{σ_z}, as well as the potentials of boundary tractions Π_{Γ} and of the Lagrange multipliers Π_{λ} are presented as follows

$$\delta\Pi_{\sigma_x} = \delta\frac{1}{2}\int_V \sigma_{xx}^{(k)^T}\varepsilon_{xx}^{(k)}dV == \frac{1}{4}\int_V \boldsymbol{\chi}_{xy}^T\mathbf{f}_{\phi}^{(k)^T}\overline{Q}_{11}^{(k)}\mathbf{f}_{\phi}^{(k)}\delta\boldsymbol{\chi}dV = \frac{1}{4}\int_L \boldsymbol{\chi}_{xy}^T\mathbf{S}_s\delta\boldsymbol{\chi}_{xy}dx, \tag{36}$$

$$\delta\Pi_c = \delta\frac{1}{2}\int_V m_{xy}^{(k)^T}\chi_{xy}^{(k)}dV = \frac{1}{4}\int_V \boldsymbol{\chi}_{xy}^T\mathbf{f}_{c_1}^{(k)^T}\tilde{Q}_{44}^{(k)}\mathbf{f}_{c_1}^{(k)}\delta\boldsymbol{\chi}dV = \frac{1}{4}\int_L \boldsymbol{\chi}_{xy}^T\mathbf{S}_{c_1}\delta\boldsymbol{\chi}_{xy}dx, \tag{37}$$

$$\delta\Pi_{\tau_{xz}} = \delta\frac{1}{2}\int_V \tau_{xz}^T\gamma_{xz}dV = \delta\frac{1}{2}\int_V\left[\mathbf{c}_{c_1}^{(k)}\boldsymbol{\chi}_{xy,x} + \hat{T}_b\right]^T\frac{1}{G_{xz}^{(k)}}\left[\mathbf{c}_{c_1}^{(k)}\boldsymbol{\chi}_{xy,x} + \hat{T}_b\right]dV$$

$$= \int_V\left[\mathbf{c}_{c_1}^{(k)}\boldsymbol{\chi}_{xy,x} + \hat{T}_b\right]^T\frac{1}{G_{xz}^{(k)}}\delta\left[\mathbf{c}_{c_1}^{(k)}\boldsymbol{\chi}_{xy,x} + \hat{T}_b\right]dV$$

$$= \int_L\left(\boldsymbol{\chi}_{xy,x}^T\left(\int_{z_0}^{z_N}\mathbf{c}_{c_1}^{(k)^T}\frac{1}{G_{xz}^{(k)}}\mathbf{c}_{c_1}^{(k)}dz\right)\delta\boldsymbol{\chi}_{xy,x} + \hat{T}_b\left[\int_{z_0}^{z_N}\frac{1}{G_{xz}^{(k)}}\mathbf{c}_{c_1}^{(k)}dz\right]\delta\boldsymbol{\chi}_{xy,x}\right)dx$$

$$= \boldsymbol{\chi}_{xy,x}^T\boldsymbol{\eta}\delta\boldsymbol{\chi}_{xy}\Big|_0^L - \int\boldsymbol{\chi}_{xy,xx}^T\boldsymbol{\eta}\delta\boldsymbol{\chi}_{xy}dx + \hat{T}_b\boldsymbol{\chi}\delta\boldsymbol{\chi}_{xy}\Big|_0^L - \int\hat{T}_{b,x}\boldsymbol{\chi}\delta\boldsymbol{\chi}_{xy}dx, \tag{38}$$

where $\boldsymbol{\eta} = \int_{z_0}^{z_N}\mathbf{c}_{c_1}^{(k)^T}\frac{1}{G_{xz}^{(k)}}\mathbf{c}_{c_1}^{(k)}dz$, $\boldsymbol{\chi} = \int_{z_0}^{z_N}\frac{1}{G_{xz}^{(k)}}\mathbf{c}_{c_1}^{(k)}dz$. (39)

$$\delta\Pi_{\sigma_z} = \delta\frac{1}{2}\int_V \sigma_z^T\varepsilon_z dV = \delta\frac{1}{2}\int_V\left[\mathbf{e}_{c_1}^{(k)}\boldsymbol{\chi}_{xy,xx} - \hat{T}_{b,x}\left(z - z_0\right) + \hat{P}_b\right]^T\left\{\begin{matrix}R_{13}^{(k)}\overline{Q}^{(k)}\mathbf{f}_{\phi}^{(k)}\boldsymbol{\chi}_{xy} \\ +R_{33}^{(k)}\left[\mathbf{e}_{c_1}^{(k)}\boldsymbol{\chi}_{xy,xx} - \hat{T}_{b,x}\left(z - z_0\right) + \hat{P}_b\right]\end{matrix}\right\}dV$$

$$= \int \boldsymbol{\chi}_{xy,xxxx}^T \boldsymbol{\rho} \delta\boldsymbol{\chi}_{xy} dx - \int \hat{T}_{b,xxx} \boldsymbol{\rho}_t \delta\boldsymbol{\chi}_{xy} dx + \int \hat{P}_{b,xx} \boldsymbol{\rho}_p \delta\boldsymbol{\chi}_{xy} dx + \frac{1}{2}\int \boldsymbol{\chi}_{xy,xx}^T \boldsymbol{\omega} \delta\boldsymbol{\chi}_{xy} dx$$

$$+ \int \frac{1}{2}\boldsymbol{\chi}_{xy,xx}^T \boldsymbol{\omega} \delta\boldsymbol{\chi}_{xy} dx - \int \frac{1}{2}\hat{T}_{b,x} \boldsymbol{\omega}_t \delta\boldsymbol{\chi}_{xy} dx + \int \frac{1}{2}\hat{P}_b \boldsymbol{\omega}_p \delta\boldsymbol{\chi}_{xy} dx$$

$$- \boldsymbol{\chi}_{xy,xxx}^T \boldsymbol{\rho} \delta\boldsymbol{\chi}_{xy}\Big|_0^L + \hat{T}_{b,xx} \boldsymbol{\rho}_t \delta\boldsymbol{\chi}_{xy}\Big|_0^L - \hat{P}_{b,x} \boldsymbol{\rho}_p \delta\boldsymbol{\chi}_{xy}\Big|_0^L - \frac{1}{2}\boldsymbol{\chi}_{xy,x}^T \boldsymbol{\omega} \delta\boldsymbol{\chi}_{xy}\Big|_0^L$$

$$+ \boldsymbol{\chi}_{xy,xx}^T \boldsymbol{\rho} \delta\boldsymbol{\chi}_{xy,x}\Big|_0^L - \hat{T}_{b,x} \boldsymbol{\rho}_t \delta\boldsymbol{\chi}_{xy,x}\Big|_0^L + \hat{P}_b \boldsymbol{\rho}_p \delta\boldsymbol{\chi}_{xy,x}\Big|_0^L + \frac{1}{2}\boldsymbol{\chi}_{xy}^T \boldsymbol{\omega} \delta\boldsymbol{\chi}_{xy,x}\Big|_0^L \tag{40}$$

where

$$\boldsymbol{\rho} = \int_{z_0}^{z_N} \mathbf{e}_{c_1}^{(k)^T} R_{33}^{(k)} \mathbf{e}^{(k)} dz, \boldsymbol{\rho}_t = \int_{z_0}^{z_N} R_{33}^{(k)} (z - z_0) \mathbf{e}_{c_1}^{(k)} dz, \boldsymbol{\rho}_p = \int_{z_0}^{z_N} R_{33}^{(k)} \mathbf{e}_{c_1}^{(k)} dz, \tag{41a}$$

$$\boldsymbol{\omega} = \int_{z_0}^{z_N} \mathbf{e}_{c_1}^{(k)^T} R_{13}^{(k)} \overline{Q}^{(k)} \mathbf{f}_{\phi}^{(k)} dz, \boldsymbol{\omega}_t = \int_{z_0}^{z_N} R_{13}^{(k)} (z - z_0) \overline{Q}^{(k)} \mathbf{f}_{\phi}^{(k)} dz, \boldsymbol{\omega}_p = \int_{z_0}^{z_N} R_{13}^{(k)} \overline{Q}^{(k)} \mathbf{f}_{\phi}^{(k)} dz. \tag{41b}$$

$$\delta\Pi_\Gamma = -\Big[\delta\left(\mathbf{S}_s \boldsymbol{\chi}_{xy}\right).\hat{\boldsymbol{\mathcal{U}}} + \delta Q \hat{w}\Big]\Big|_0^L = -\Big[\hat{\boldsymbol{\mathcal{U}}} \mathbf{S}_{sN} \delta\boldsymbol{\chi}_{xy} + \hat{w} \mathbf{S}_{sM} \delta\boldsymbol{\chi}_{xy,x}\Big]\Big|_0^L \tag{42}$$

$$\delta\Pi_\lambda = \int \Big[\mathbf{S}_{sN} \boldsymbol{\chi}_{xy,x} + \left(\hat{T}_t - \hat{T}_b\right)\Big] \delta\lambda_1 dx - \int \lambda_{1,x} \mathbf{S}_{sN} \delta\boldsymbol{\chi}_{xy} dx + \lambda_1 \mathbf{S}_{sN} \delta\boldsymbol{\chi}_{xy}\Big|_0^L$$

$$+ \int \Big[\left(\mathbf{S}_{sM} + \mathbf{S}_{c_1 M}\right) \boldsymbol{\chi}_{xy,xx} + \left(z_N \hat{T}_{t,x} - z_0 \hat{T}_{b,x}\right) + \left(\hat{P}_t - \hat{P}_b\right)\Big] \delta\lambda_2 dx$$

$$+ \Big[\lambda_2 \left(\mathbf{S}_{sM} + \mathbf{S}_{c_1 M}\right) \delta\boldsymbol{\chi}_{xy,x}\Big]\Big|_0^L - \Big[\lambda_{2,x} \left(\mathbf{S}_{sM} + \mathbf{S}_{c_1 M}\right) \delta\boldsymbol{\chi}_{xy}\Big|\Big]_0^L + \int \lambda_{2,xx} \left(\mathbf{S}_{sM} + \mathbf{S}_{c_1 M}\right) \delta\boldsymbol{\chi}_{xy} dx \tag{43}$$

Substituting Eqs. (36-43) into Eq. (35) and collecting the corresponding terms of $\delta\lambda_1$, $\delta\lambda_2$ and $\delta\boldsymbol{\chi}_{xy}$, the governing equations are obtained as following

$$\delta\lambda_1 : \mathbf{S}_{sN} \boldsymbol{\chi}_{xy,x} + \left(\hat{T}_t - \hat{T}_b\right) = 0, \tag{44a}$$

$$\delta\lambda_2 : \left(\mathbf{S}_{sM} + \mathbf{S}_{c_1 M}\right) \boldsymbol{\chi}_{xy,xx} + \left(z_N \hat{T}_{t,x} - z_0 \hat{T}_{b,x}\right) + \left(\hat{P}_t - \hat{P}_b\right) = 0, \tag{44b}$$

$$\delta\boldsymbol{\chi}_{xy} : \boldsymbol{\chi}_{xy}^T \left(\mathbf{S}_s + \frac{1}{4}\mathbf{S}_{c_1}\right) - \boldsymbol{\chi}_{xy,xx}^T \left(\boldsymbol{\eta} - \boldsymbol{\omega}\right) + \boldsymbol{\chi}_{xy,xxxx}^T \boldsymbol{\rho} + \left(\lambda_{2,xx} - \lambda_{1,x}\right) \Lambda_{eq}$$

$$= \hat{T}_{b,x} \left(\boldsymbol{\chi} + \frac{\boldsymbol{\omega}_t}{2}\right) + \hat{T}_{b,xxx} \boldsymbol{\rho}_t - \hat{P}_b \frac{\boldsymbol{\omega}_p}{2} - \hat{P}_{b,xx} \boldsymbol{\rho}_p, \tag{44c}$$

where

$$\mathbf{S}_{sN} = \mathbf{S}_s(1,:) \text{ (the first row of } \mathbf{S}_s\text{)}, \ \mathbf{S}_{sM} = \mathbf{S}_s(2,:) \text{ (the second row of } \mathbf{S}_s\text{)}, \tag{45a}$$

$$\mathbf{S}_{c_1 M} = \frac{1}{2}\sum_{k=1}^{N} \tilde{Q}_{44}^{(k)} \mathbf{g}_{c_1}^{(k)}, \text{ and } T \text{ denotes the transpose of matrix.} \tag{45b}$$

The pertinent boundary conditions are given by

$$\delta\boldsymbol{\chi}_{xy} = 0 \text{ or } \boldsymbol{\chi}_{xy,x}^T \left(\boldsymbol{\eta} - \frac{\boldsymbol{\omega}}{2}\right) - \boldsymbol{\chi}_{xy,xxx}^T \boldsymbol{\rho} + \left(\lambda_1 - \lambda_{2,x}\right) \Lambda_{bc} = \hat{\boldsymbol{\mathcal{U}}} - \hat{T}_b \boldsymbol{\chi} - \hat{T}_{b,xx} \boldsymbol{\rho}_t + \hat{P}_{b,x} \boldsymbol{\rho}_p, \tag{46a}$$

$$\delta\boldsymbol{\chi}_{xy,x}=0 \text{ or } \boldsymbol{\chi}_{xy}^{T}\frac{\boldsymbol{\omega}}{2}+\boldsymbol{\chi}_{xy,xx}^{T}\boldsymbol{\rho}-\hat{T}_{b,x}\boldsymbol{\rho}_{t}+\lambda_{2}\Lambda_{bc}=\widehat{\mathcal{W}}+\hat{T}_{b,x}\boldsymbol{\rho}_{t}-\hat{P}_{b}\boldsymbol{\rho}_{p}, \tag{46b}$$

$$\text{where } \Lambda_{eq}=\Lambda_{bc}=\begin{bmatrix}1 & 1 & 1 & 1 & 1 & 1\end{bmatrix}^{T}. \tag{47}$$

These governing equations are developed based on the strain-displacement formulation within the framework of the modified couple stress theory, hence denoted by SD MCS in Section 3 detailing numerical results and discussions. The model excluding couple stress can be readily obtained by removing the term $w_{0,xx}$ in $\boldsymbol{\chi}_{xy}$ and the corresponding row and column in Eqs. (44) and (46). Finally, the differential quadrature method [75] is used to solve the algebraic equations in Eqs. (44) and (46).

3. Numerical results and discussions

The validation of strain-displacement mixed variational formulations developed in Section 2 is assessed for a number of laminated beams. Section 3.1 presents the first validation of the present strain-displacement formulation as compared to the closed-form 3D solution by Pagano [79] and the Hellinger-Reissner (HR) mixed formulation by Groh and Weaver [41] for simply-supported laminates. It is shown that the proposed strain-displacement mixed formulations predict the displacement and stress components well in comparison with those obtained from the HR principle and the exact solution. Next, the role of couple stress in capturing localised stresses near the clamped boundary is discussed in Section 3.2. While the shear stress and transverse normal stress are predicted well by both strain-displacement models, the model with an additional curvature introduced by the couple stress provides more functional freedom in minimising the energy, hence, calculates more accurately the deflection and axial stress compared with the model in which the couple stress is excluded. In this section, the effect of length scales to the optimised strain energy in flexural behaviours of laminated beams is also discussed. For verification purpose, the displacement and stresses are normalised as follows

$$\bar{w}=\frac{10^{6}t^{2}}{q_{0}L^{4}}u_{z},\ \bar{\sigma}_{x}=\frac{t^{2}}{q_{0}L^{2}}\sigma_{x},\ \bar{\tau}_{xz}=\frac{\tau_{xz}}{q_{0}},\ \bar{\sigma}_{z}=\frac{\sigma_{z}}{q_{0}}.$$

3.1. Model validation

The present strain-displacement mixed formulation is firstly validated for relatively thick laminates with the length-to-thickness ratio being $L/t=8$. The beam axis is aligned with the Cartesian x-direction, while the z-direction is the thickness-wise axis. A sinusoidal distributed load is divided equally between the top and bottom surfaces, $\hat{P}_t$=$\hat{P}_b=-q_0/2\,sin(\pi x/L)$, while both ends are simply supported as shown in Fig. 2. A number of stacking sequences proposed by Groh and Weaver [41] are used to test the present mixed formulation. The laminates are separated into the symmetric layups A-H and the non-symmetric layups I-M as in Table 1. In the paper by Groh and Weaver [41], different materials with significant changes in mechanical properties were used to demonstrate the capacity of the Hellinger-Reissner mixed formulation. These materials are reproduced in Table 2 for the present study. Material p represents a fibre-reinforced plastic material, whereas material m is the representative of a transversely stiff material. Material pvc represents a poly-vinyl chloride isotropic foam and material h is a soft

honeycomb core modelled as a transversely isotropic material to magnify the zigzag effect. Using these materials, different structures proposed in [41] are represented for numerical testing. Laminates A-D are symmetric cross-ply laminates with equal ply thickness, assembled by various number of plies: Laminates A and B are made of three and five layers with 0^0 plies at top and bottom, Laminate D is a challenging test case of equivalent single layer (ESL) model due to a numerous sharp changes of mechanical properties with 51 alternatively $0^0/90^0$ plies; and Laminate C is a counterpart of Laminate B to consider the Externally Weak Layer (EWL) effect [80]. Symmetric layups E-G are soft thick-core sandwich laminates with rapid variation of material properties in the skin layers, while Laminate H can be considered as a hard-core sandwich in which the material properties vary sharply in the core area. The numerical test is also performed for non-symmetric Laminates I-M. Laminates I and J are the anti-symmetric correspondents of the above-mentioned Laminates A-D, while Laminates K-M are highly heterogeneous beams with general ply orientations, thickness and material properties.

The relative errors for the present results compared against the 3D exact solution given by Pagano is presented in Table 3. The corresponding Figs. 3-19 depict the through-thickness axial stress and transverse normal stress at the midspan as well as the shear stress at the left end of the beams. It is worth noting that Pagano's solution was developed for the cylindrical bending of an infinite wide plate [75]; therefore, the results herein are obtained by applying the plane strain condition in the material stiffness matrix as specified by Patni and co-workers [81]. The HR3-RZT developed by Groh and Weaver [41] based on the Hellinger-Reissner mixed variational solution and the same third-order zigzag kinematics as employed in this work, is also regenerated herein for verification purpose. The numerical data obtained from the strain-displacement formulation developed within the framework of the modified couple stress theory is denoted by SD MCS, whereas model SD stands for its reduced model neglecting the couple stress in the equilibrium equations. It is worth noting that in the modified couple stress theory the couple stress is negligible if the length scale is set to be very small compared to the structural dimensions; therefore, the length scale is set to be $t/l = 10^9$ for the results in this table. It is shown that the two strain-displacement mixed formulations perform very well in capturing the deflection, axial and transverse shear stresses of the considered laminates. For the symmetric laminates, the accuracy of both models for the normalised deflection w is within 0.64% in comparison to Pagano's solution. With respect to the stress analysis, the Hellinger-Reissner principle giving rise to the independence of stress resultants and displacement variables provides a better prediction of the axial stress and transverse shear stress for symmetric laminates in comparison with the present mixed models, which are solved for strain and displacement functional unknowns. The errors are within 1.24% for axial stress and 2.62% for shear stress of Laminates C, E, F, G, H. However, a higher error is observed for Laminate D, which may be caused by the insufficient assumed kinematic field for this 51-cross-ply layup. On the other hand, for the non-symmetric laminates, there is a compromise of accuracy for axial and shear stresses compared against the stress-displacement mixed formulation (HR model). That is the present strain-displacement formulations are less accurate in capturing the axial stress but predict better the shear stress in comparison with the HR counterpart. In these laminates, the deflections obtained from both strain-displacement formulations agree well with those from the Hellinger-Reissner mixed formulations and the 3D exact solution, except that the SD model predicts a slightly stiffer behaviour for Laminate I, where the error

for w is -2.3%. It is worth noting that the present solution does not require a post-processing stress recovery steps thanks to the enforcement of Cauchy's equilibrium conditions in the stress assumptions, which is similar to the approach presented in the Hellinger-Reissner mixed formulations by Groh and Weaver [41].

3.2. Localised stresses near the clamped boundary

In this section, a further verification is carried out for the strain-displacement formulations developed herein. A clamped beam with the length-to-thickness ratio of $L/t = 10$ is loaded by uniform pressure on the top and bottom surface, i.e. $\hat{P}_t$=$\hat{P}_b = -q_0/2$, as described in Fig. 20. The stacking sequence is [0/90/0/90] with equal ply thickness of material *p*. The results obtained from the two strain-displacement models are compared with a 3D Abaqus solution presented in [75, 81] as well as the HR3-RZT solution developed in [41]. Figs. 21-23 present the normalised axial stress $\bar{\sigma}_x$, transverse shear stress $\bar{\tau}_{xz}$ and normal stress $\bar{\sigma}_z$ at four locations distanced 5%, 10%, 15% and 20% of the span from the clamped end ($x = 0$). In this area, both the stress-channelling and the zigzag effect are observed due to the strong boundary effect and the high orthotropy of laminae. Therefore, investigating the stress metrics in this region is crucial for the justification of different models using the same assumed kinematics, *i.e.* SD, SD MCS and HR3-RZT, in fulfilling the equilibrium conditions and minimising the structural energy. As can be seen in Figs. 22 and 23 for the transverse shear and normal stresses from locations 15% and 20%, the stress fields are more stable due to the smaller effect from the clamped boundary.

It is observed that the strain-displacement (SD) model without couple stress, which is equivalent to HR3-RZT in terms of through-thickness kinematics assumption, fails to capture the axial stress near the boundary. This means that the stress-displacement HR model allows better possibility of minimising the energy in comparison with the strain-displacement counterpart. Meanwhile, the strain-displacement (SD MCS) model developed in the framework of the modified couple stress significantly improves the prediction of the stresses compared to the SD model. This is due to the presence of the additional curvature $w_{0,xx}$ in the governing equation, which provides more functional freedom to minimise the total strain energy. It is worth mentioning that, the curvature $w_{0,xx}$ mainly contributes to the optimisation of the longitudinal profiles while holding the strong constitutive and strain-displacement relations over the cross-section. Furthermore, changing the length scale parameters is equivalent to seeking an optimised strain energy contribution of $w_{0,xx}$ in the total strain energy by varying the stiffness $\tilde{Q}_{44}^{(k)}$ relating to the couple stress in Eq. 12. An investigation of the effect of these length scales in the optimised energy is presented in Fig. 24 to compare with the strain energy in the SD and HR3 RZT models. The thickness-to-length scale ratio is chosen to be 20, 25, 50 and 10^9 corresponding to the decrease of the length scales with regards to the beam thickness. For example, if $t/l = 10^9$ the length scale is small compared to the thickness, which means that the couple stress is marginal in comparison with other stress components. By using the SD model, the optimum strain energy is higher compared to the HR3 RZT model, which explains the inability of the SD model in capturing the axial stress mentioned previously. However, as the couple stress is included in the SD MCS model, the energy can be optimised better. It is also shown that with the present kinematic assumptions, small length scales provide better converged

results and more optimised strain energy. In order to improve the accuracy of the SD MCS model, higher-order kinematics is needed to fulfil the complex displacement fields near the boundary.

4. Conclusions

The aim of this paper is to develop a strain-displacement (SD) mixed formulation to analyse the bending behaviour of laminated beams. Based on an equivalent single layer approach, third-order global and linear zigzag kinematics is assumed over the cross-section for the axial displacement to effectively model stress channelling effects due to material orthotropy and the zigzag effect originating from differences in shear strains at layer interfaces. The shear stress and the transverse normal stress are calculated from the equilibrium condition so that they can be captured accurately *a priori* if the axial stress is fully described. Following the approach initially applied to the Hellinger-Reissner principle by Groh and Weaver [41], the Lagrange multipliers corresponding to the axial and transverse displacements are used to enforce the equilibrium conditions in the equivalent single layer model, which results in a mixed formulation of strains and displacements in this SD model rather than stress resultants and displacements presented in [41]. Furthermore, couple stress is included to enrich the functional unknowns in minimising the strain energy, which leads to a strain-displacement formulation within the framework of the modified couple stress theory denoted by SD MCS.

The numerical results reveal that both the SD and SD MCS models can accurately predict the flexural behaviour of various simply-supported beams including symmetric and antisymmetric laminates, as well as thick-soft core sandwich beams. With respect to localised stresses near clamped boundaries, the curvature $w_{0,xx}$ appearing from the couple stress measure significantly improves the accuracy of the solution. It is common in the literature [78, 82, 83] to conclude that the length scales associated with the couple-stress constitutive relation is a parameter to capture the size effects generated by sub-scales and that the solution of couple-stress-based theory recovers the Cauchy-based solution if the length scales becomes very small. However, in this strain-displacement mixed formulation, the couple stress also provides an extra parameter to minimise the strain energy so that the macro structural behaviour can be predicted more accurately, which is not possible in the Cauchy counterpart, *i.e.* the SD model. Using the optimised strain energy as an index to evaluate the accuracy of the numerical solution, the variable length scale can be investigated as a factor to improve the performance of the modified couple stress-based strain-displacement formulation. The optimised length scale for different structures with this modified couple stress-based strain-displacement formulation, however, requires further investigation.

Acknowledgments

L.C. Trinh, G. Zucco and P.M. Weaver would like to acknowledge funding from the Science Foundation Ireland (SFI) for the award of a Research Professor grant (Varicomp: 15/RP/2773). R.M.J. Groh is supported by the Royal Academy of Engineering under the Research Fellowship scheme [Grant No. RF/201718/17178].

Appendices

Appendix 1: Enforcing the interlaminar and surfaces conditions for shear stress to obtain the constant vector $\mathbf{a}^{(k)}$:

Layer 1, z=z$_0$:

$$\tau_{xz}^{(1)}\Big|_{z=z_0} = \hat{T}_b = \left[-\overline{Q}_{11}^{(1)}\mathbf{g}_{\phi}^{(1)}(z_0) + \frac{1}{4}\overline{Q}_{44}^{(1)}\mathbf{f}_{c_1}^{(1)}(z_0)\right]\boldsymbol{\chi}_{xy,x} + \mathbf{a}^{(1)} \tag{A1.1}$$

$$\therefore \mathbf{a}^{(1)} = \left[\overline{Q}_{11}^{(1)}\mathbf{g}_{\phi}^{(1)}(z_0) - \frac{1}{4}\tilde{Q}_{44}^{(1)}\mathbf{f}_{c_1}^{(1)}(z_0)\right]\boldsymbol{\chi}_{xy,x} + \hat{T}_b \tag{A1.2}$$

Layer 1, z=z$_1$:

$$\tau_{xz}^{(1)}\Big|_{z=z_1} = \left[-\overline{Q}_{11}^{(1)}\mathbf{g}_{\phi}^{(1)}(z_1) + \frac{1}{4}\tilde{Q}_{44}^{(1)}\mathbf{f}_{c_1}^{(1)}(z_1)\right]\boldsymbol{\chi}_{xy,x} + \mathbf{a}^{(1)} \tag{A1.3}$$

Layer 2, z=z$_1$:

$$\tau_{xz}^{(2)}\Big|_{z=z_1} = \left[-\overline{Q}_{11}^{(2)}\mathbf{g}_{\phi}^{(2)}(z_1) + \frac{1}{4}\tilde{Q}_{44}^{(2)}\mathbf{f}_{c_1}^{(2)}(z_1)\right]\boldsymbol{\chi}_{xy,x} + \mathbf{a}^{(2)} \tag{A1.4}$$

The interlaminar condition requires $\tau_{xz}^{(1)}\Big|_{z=z_1} = \tau_{xz}^{(2)}\Big|_{z=z_1}$:

$$\left[-\overline{Q}_{11}^{(1)}\mathbf{g}_{\phi}^{(1)}(z_1) + \frac{1}{4}\tilde{Q}_{44}^{(1)}\mathbf{f}_{c_1}^{(1)}(z_1)\right]\boldsymbol{\chi}_{xy,x} + \mathbf{a}^{(1)} = \left[-\overline{Q}_{11}^{(2)}\mathbf{g}_{\phi}^{(2)}(z_1) + \frac{1}{4}\tilde{Q}_{44}^{(2)}\mathbf{f}_{c_1}^{(2)}(z_1)\right]\boldsymbol{\chi}_{xy,x} + \mathbf{a}^{(2)} \tag{A1.5}$$

Substitute $\mathbf{a}^{(1)}$ from Eq. (A1.2) and note that $\overline{Q}_{11}^{(0)} = 0$ and $\tilde{Q}_{44}^{(0)} = 0$, one obtains:

$$\begin{aligned}\mathbf{a}^{(2)} &= \mathbf{a}^{(1)} + \left[\left(\overline{Q}_{11}^{(2)}\mathbf{g}_{\phi}^{(2)}(z_1) - \overline{Q}_{11}^{(1)}\mathbf{g}_{\phi}^{(1)}(z_1)\right) - \left(\frac{1}{4}\tilde{Q}_{44}^{(2)}\mathbf{f}_{c_1}^{(2)}(z_1) - \frac{1}{4}\tilde{Q}_{44}^{(1)}\mathbf{f}_{c_1}^{(1)}(z_1)\right)\right]\boldsymbol{\chi}_{xy,x} \\ &= \left[\left(\overline{Q}_{11}^{(1)}\mathbf{g}_{\phi}^{(1)}(z_0) - \overline{Q}_{11}^{(0)}\mathbf{g}_{\phi}^{(0)}(z_0)\right) - \left(\frac{1}{4}\tilde{Q}_{44}^{(1)}\mathbf{f}_{c_1}^{(1)}(z_0) - \frac{1}{4}\tilde{Q}_{44}^{(0)}\mathbf{f}_{c_1}^{(0)}(z_0)\right)\right]\boldsymbol{\chi}_{xy,x} + \hat{T}_b \\ &+ \left[\left(\overline{Q}_{11}^{(2)}\mathbf{g}_{\phi}^{(2)}(z_1) - \overline{Q}_{11}^{(1)}\mathbf{g}_{\phi}^{(1)}(z_1)\right) - \left(\frac{1}{4}\tilde{Q}_{44}^{(2)}\mathbf{f}_{c_1}^{(2)}(z_1) - \frac{1}{4}\tilde{Q}_{44}^{(1)}\mathbf{f}_{c_1}^{(1)}(z_1)\right)\right]\boldsymbol{\chi}_{xy,x}\end{aligned} \tag{A1.6}$$

The generic constant at kth layer

$$\begin{aligned}\mathbf{a}^{(k)} &= \left[\sum_{i=1}^{k}\left(\overline{Q}_{11}^{(i)}\mathbf{g}_{\phi}^{(i)}(z_{i-1}) - \overline{Q}_{11}^{(i-1)}\mathbf{g}_{\phi}^{(i-1)}(z_{i-1})\right) - \frac{1}{4}\sum_{i=1}^{k}\left(\tilde{Q}_{44}^{(i)}\mathbf{f}_{c_1}^{(i)}(z_{i-1}) - \tilde{Q}_{44}^{(i-1)}\mathbf{f}_{c_1}^{(i-1)}(z_{i-1})\right)\right]\boldsymbol{\chi}_{xy,x} + \hat{T}_b \\ &= \boldsymbol{\alpha}_s^{(k)}\boldsymbol{\chi}_{xy,x} + \hat{T}_b\end{aligned} \tag{A1.7}$$

Appendix 2: Enforcing the interlaminar and surfaces conditions for transverse normal stress to obtain the constant vector $\mathbf{b}^{(k)}$

Layer 1, z=z$_0$:

$$\sigma_{z=z_0}^{(1)} = \hat{P}_b = \left[\left(\overline{Q}_{11}^{(1)}\mathbf{h}_{\phi}^{(1)}(z_0) - \boldsymbol{\alpha}_s^{(1)} z_0\right) - \left(\frac{1}{2}\tilde{Q}_{44}^{(1)}\mathbf{g}_{c_1}^{(1)}(z_0) + \boldsymbol{\alpha}_{c_1}^{(1)} z_0\right)\right]\boldsymbol{\chi}_{xy,xx} - \hat{T}_{b,x} z_0 + \mathbf{b}^{(1)} \tag{A2.1}$$

$$\therefore \mathbf{b}^{(1)} = \left[-\left(\overline{Q}_{11}^{(1)}\mathbf{h}_{\phi}^{(1)}(z_0) - \boldsymbol{\alpha}_s^{(1)} z_0\right) + \left(\frac{1}{2}\tilde{Q}_{44}^{(1)}\mathbf{g}_{c_1}^{(1)}(z_0) + \boldsymbol{\alpha}_{c_1}^{(1)} z_0\right)\right]\boldsymbol{\chi}_{xy,xx} + \hat{T}_{b,x} z_0 + \hat{P}_b \tag{A2.2}$$

Layer 1, z=z$_1$:

$$\sigma_{z=z_1}^{(1)} = \left[\left(\overline{Q}_{11}^{(1)}\mathbf{h}_{\phi}^{(1)}(z_1) - \boldsymbol{\alpha}_s^{(1)} z_1\right) - \left(\frac{1}{2}\tilde{Q}_{44}^{(1)}\mathbf{g}_{c_1}^{(1)}(z_1) + \boldsymbol{\alpha}_{c_1}^{(1)} z_1\right)\right]\boldsymbol{\chi}_{xy,xx} - \hat{T}_{b,x} z_1 + \mathbf{b}^{(1)} \tag{A2.3}$$

Layer 2, z=z$_1$:

$$\sigma_{z=z_1}^{(2)} = \left[\left(\overline{Q}_{11}^{(2)}\mathbf{h}_{\phi}^{(2)}(z_1) - \boldsymbol{\alpha}_s^{(2)} z_1\right) - \left(\frac{1}{2}\tilde{Q}_{44}^{(2)}\mathbf{g}_{c_1}^{(2)}(z_1) + \boldsymbol{\alpha}_{c_1}^{(2)} z_1\right)\right]\boldsymbol{\chi}_{xy,xx} - \hat{T}_{b,x} z_1 + \mathbf{b}^{(2)} \tag{A2.4}$$

Interlaminar condition requires $\sigma_z^{(1)}\big|_{z=z_1} = \sigma_z^{(2)}\big|_{z=z_1}$ such that,

$$\begin{aligned}
&\left[\left(\overline{Q}_{11}^{(2)}\mathbf{h}_{\phi}^{(2)}(z_1) - \boldsymbol{\alpha}_s^{(2)} z_1\right) - \left(\frac{1}{2}\tilde{Q}_{44}^{(2)}\mathbf{g}_{c_1}^{(2)}(z_1) + \boldsymbol{\alpha}_{c_1}^{(2)} z_1\right)\right]\boldsymbol{\chi}_{xy,xx} - \hat{T}_{b,x} z_1 + \mathbf{b}^{(2)} \\
&= \left[\left(\overline{Q}_{11}^{(1)}\mathbf{h}_{\phi}^{(1)}(z_1) - \boldsymbol{\alpha}_s^{(1)} z_1\right) - \left(\frac{1}{2}\tilde{Q}_{44}^{(1)}\mathbf{g}_{c_1}^{(1)}(z_1) + \boldsymbol{\alpha}_{c_1}^{(1)} z_1\right)\right]\boldsymbol{\chi}_{xy,xx} - \hat{T}_{b,x} z_1 + \mathbf{b}^{(1)}
\end{aligned} \tag{A2.5}$$

Substitute $\mathbf{b}^{(1)}$ from Eq. (A2.2) and note that $\overline{Q}_{11}^{(0)} = 0$ and $\tilde{Q}_{44}^{(0)} = 0$, one obtains:

$$\begin{aligned}
\mathbf{b}^{(2)} &= \mathbf{b}^{(1)} - \left\{\left[\overline{Q}_{11}^{(2)}\mathbf{h}_{\phi}^{(2)}(z_1) - \overline{Q}_{11}^{(1)}\mathbf{h}_{\phi}^{(1)}(z_1)\right] - \left(\boldsymbol{\alpha}_s^{(2)} - \boldsymbol{\alpha}_s^{(1)}\right) z_1\right\}\boldsymbol{\chi}_{xy,xx} \\
&+ \left\{\frac{1}{2}\left[\tilde{Q}_{44}^{(2)}\mathbf{g}_{c_1}^{(2)}(z_1) - \tilde{Q}_{44}^{(1)}\mathbf{g}_{c_1}^{(1)}(z_1)\right] + \left(\boldsymbol{\alpha}_{c_1}^{(2)} - \boldsymbol{\alpha}_{c_1}^{(1)}\right) z_1\right\}\boldsymbol{\chi}_{xy,xx} \\
&= \left[-\left(\overline{Q}_{11}^{(1)}\mathbf{h}_{\phi}^{(1)}(z_0) - \boldsymbol{\alpha}_s^{(1)} z_0\right) + \left(\frac{1}{2}\tilde{Q}_{44}^{(1)}\mathbf{g}_{c_1}^{(1)}(z_0) + \boldsymbol{\alpha}_{c_1}^{(1)} z_0\right)\right]\boldsymbol{\chi}_{xy,xx} + \hat{T}_{b,x} z_0 + \hat{P}_b \\
&+ \left\{\begin{array}{l}
-\left[\left(\overline{Q}_{11}^{(2)}\mathbf{h}_{\phi}^{(2)}(z_1) - \overline{Q}_{11}^{(1)}\mathbf{h}_{\phi}^{(1)}(z_1)\right) - \left(\boldsymbol{\alpha}_s^{(2)} - \boldsymbol{\alpha}_s^{(1)}\right) z_1\right] \\
+\left[\left(\frac{1}{2}\tilde{Q}_{44}^{(2)}\mathbf{g}_{c_1}^{(2)}(z_1) - \frac{1}{2}\tilde{Q}_{44}^{(1)}\mathbf{g}_{c_1}^{(1)}(z_1)\right) + \left(\boldsymbol{\alpha}_{c_1}^{(2)} - \boldsymbol{\alpha}_{c_1}^{(1)}\right) z_1\right]
\end{array}\right\}\boldsymbol{\chi}_{xy,xx}
\end{aligned} \tag{A2.6}$$

The generic constant at kth layer

$$\mathbf{b}^{(k)} = \sum_{i=1}^{k} \left\{ \begin{array}{l} -\left[\left(\overline{Q}_{11}^{(i)} \mathbf{h}_{\phi}^{(i)} \left(z_{i-1} \right) - \overline{Q}_{11}^{(i-1)} \mathbf{h}_{\phi}^{(i-1)} \left(z_{i-1} \right) \right) - \left(\boldsymbol{\alpha}_{s}^{(i)} - \boldsymbol{\alpha}_{s}^{(i-1)} \right) z_{i-1} \right] \\ + \left[\frac{1}{2} \left(\tilde{Q}_{44}^{(i)} \mathbf{g}_{c_1}^{(i)} \left(z_{i-1} \right) - \tilde{Q}_{44}^{(i-1)} \mathbf{g}_{c_1}^{(i-1)} \left(z_{i-1} \right) \right) + \left(\boldsymbol{\alpha}_{c_1}^{(i)} - \boldsymbol{\alpha}_{c_1}^{(i-1)} \right) z_{i-1} \right] \end{array} \right\} \boldsymbol{\chi}_{xy,xx} + \hat{T}_{b,x} z_0 + \hat{P}_b$$

$$= \boldsymbol{\beta}_{s}^{(k)} \boldsymbol{\chi}_{xy,xx} + \hat{T}_{b,x} z_0 + \hat{P}_b \qquad \text{(A2.7)}$$

List of tables

List of figures

Table 1: Mechanical properties of h, p, m and pvc normalised by the in-plane modulus $\boldsymbol{G_{12}^{(h)}}$ of h.

Material	$\frac{E_1}{G_{12}^{(h)}}$	$\frac{E_2}{G_{12}^{(h)}}$	$\frac{E_3}{G_{12}^{(h)}}$	$\frac{G_{12}}{G_{12}^{(h)}}$	$\frac{G_{13}}{G_{12}^{(h)}}$	$\frac{G_{23}}{G_{12}^{(h)}}$	ν_{12}	ν_{13}	ν_{23}
h	250.0	250.0	2500.0	1.0	875.0	1750.0	0.9	3.0×10^{-5}	3.0×10^{-5}
p	25.0×10^{6}	1.0×10^{6}	1.0×10^{6}	5.0×10^{5}	5.0×10^{5}	2.0×10^{5}	0.25	0.25	0.25
m	32.57×10^{6}	1.0×10^{6}	10.0×10^{6}	6.5×10^{5}	8.21×10^{6}	3.28×10^{6}	0.25	0.25	0.25
pvc	25.0×10^{4}	25.0×10^{4}	25.0×10^{4}	9.62×10^{4}	9.62×10^{4}	9.62×10^{4}	0.3	0.3	0.3

Table 2: Stacking sequence for laminates under simply-supported boundaries. The subscripts determine the number of laminae replicating the pertinent property.

Laminate	Layer thickness ratio	Layer materials	Stacking sequence
Symmetric			
A	$[(1/3)_3]$	$[p_3]$	[0/90/0]
B	$[0.2_5]$	$[p_5]$	[0/90/0/90/0]
C	$[0.2_5]$	$[p_5]$	[90/0/90/0/90]
D	$[(1/51)_{51}]$	$[p_{51}]$	$[0/(90/0)_{25}]$
E	$[(1/30)_3/0.8/(1/30)_3]$	$[p_3/pvc/p_3]$	$[0/90/0_3/90/0]$
F	$[(1/30)_3/0.8/(1/30)_3]$	$[p_3/h/p_3]$	$[0/90/0_3/90/0]$
G	$[0.1_2/0.2_3/0.1_2]$	$[p_2/pvc/h/pvc/p_2]$	$[90/0_5/90]$
H	$[(1/12)_{12}]$	$[p_{12}]$	$[\pm 45/\mp 45/0/90_2/0/\mp 45/\pm 45]$
Asymmetric			
I	[0.3/0.7]	$[p_2]$	[0/90]
J	$[0.25_4]$	$[p_4]$	[0/90/0/90]
K	[0.1/0.3/0.35/0.25]	$[p_2/m/p]$	$[0/90/0_2]$
L	[0.3/0.2/0.15/0.25/0.1]	$[p_3/m/p]$	$[0/90/0_2/90]$
M	[0.1/0.7/0.2]	[m/pvc/p]	$[0_3]$

Table 3: Normalised maximum deflection, maximum axial stress and shear stress for simply-supported laminates. Different results are specified by percentage errors in comparison with Pagano's solution.

Laminate	Model	$\bar{w}$		$\bar{\sigma}_x^{max}$		$\bar{\tau}_{xz}^{max}$	
A	**Pagano**	**0.0116**		**0.7913**		**3.3167**	
	HR3-RZT	0.0116	**(-0.01)**	0.7895	**(-0.23)**	3.3155	**(-0.04)**
	SD MCS	0.0116	**(0.26)**	0.7702	**(-2.66)**	3.3112	**(-0.17)**
	SD	0.0116	**(0.26)**	0.7616	**(-3.75)**	3.3102	**(-0.20)**
B	**Pagano**	**0.0124**		**0.8672**		**3.3228**	
	HR3-RZT	0.0124	**(0.00)**	0.8593	**(-0.92)**	3.3206	**(-0.07)**
	SD MCS	0.0125	**(0.25)**	0.8357	**(-3.63)**	3.3198	**(-0.09)**
	SD	0.0125	**(0.25)**	0.8357	**(-3.64)**	3.3177	**(-0.15)**
C	**Pagano**	**0.0303**		**1.6307**		**5.3340**	
	HR3-RZT	0.0303	**(0.15)**	1.6226	**(-0.49)**	5.3361	**(0.04)**
	SD MCS	0.0304	**(0.22)**	1.6361	**(0.33)**	5.3369	**(0.05)**
	SD	0.0304	**(0.22)**	1.6361	**(0.33)**	5.3317	**(-0.04)**
D	**Pagano**	**0.0154**		**1.2239**		**3.6523**	
	HR3-RZT	0.0154	**(0.03)**	1.2280	**(0.34)**	3.6505	**(-0.05)**
	SD MCS	0.0155	**(0.52)**	1.1169	**(-8.74)**	3.7622	**(3.01)**
	SD	0.0155	**(0.52)**	1.1171	**(-8.73)**	3.7660	**(3.11)**
E	**Pagano**	**0.0309**		**1.9593**		**2.8329**	
	HR3-RZT	0.0309	**(-0.02)**	1.9596	**(0.02)**	2.8300	**(-0.10)**
	SD MCS	0.0310	**(0.20)**	1.9835	**(1.24)**	2.8435	**(0.37)**
	SD	0.0310	**(0.20)**	1.9837	**(1.24)**	2.8290	**(-0.14)**
F	**Pagano**	**1.0645**		**13.9883**		**8.1112**	
	HR3-RZT	1.0615	**(-0.28)**	13.9545	**(-0.24)**	8.1155	**(0.05)**
	SD MCS	1.0645	**(0.00)**	13.9523	**(-0.26)**	8.1702	**(0.73)**
	SD	1.0645	**(0.00)**	13.9496	**(-0.28)**	8.1160	**(0.06)**
G	**Pagano**	**0.4590**		**6.3417**		**5.6996**	
	HR3-RZT	0.4589	**(-0.02)**	6.3431	**(0.02)**	5.7014	**(0.03)**
	SD MCS	0.4591	**(0.02)**	6.3421	**(0.01)**	5.7050	**(0.10)**
	SD	0.4591	**(0.02)**	6.3421	**(0.01)**	5.7034	**(0.07)**
H	**Pagano**	**0.0224**		**0.6157**		**4.0096**	
	HR3-RZT	0.0225	**(0.51)**	0.6173	**(0.27)**	4.0117	**(0.05)**
	SD MCS	0.0225	**(0.64)**	0.6106	**(-0.84)**	4.1148	**(2.62)**
	SD	0.0225	**(0.64)**	0.6105	**(-0.84)**	4.0980	**(2.20)**
I	**Pagano**	**0.0482**		**2.0870**		**4.8797**	
	HR3-RZT	0.0484	**(0.35)**	2.0726	**(-0.69)**	4.7952	**(-1.73)**
	SD MCS	0.0482	**(0.06)**	2.0193	**(-3.24)**	4.8889	**(0.19)**
	SD	0.0471	**(-2.30)**	2.0191	**(-3.25)**	4.8886	**(0.18)**
J	**Pagano**	**0.0195**		**1.2175**		**4.3539**	
	HR3-RZT	0.0196	**(0.45)**	1.2064	**(-0.92)**	4.4680	**(2.62)**
	SD MCS	0.0195	**(0.24)**	1.1783	**(-3.22)**	4.3480	**(-0.14)**
	SD	0.0195	**(-0.11)**	1.1781	**(-3.24)**	4.3161	**(-0.87)**
K	**Pagano**	**0.0100**		**0.9566**		**4.1236**	
	HR3-RZT	0.0100	**(0.14)**	0.9526	**(-0.41)**	4.1877	**(1.56)**
	SD MCS	0.0100	**(0.33)**	0.9678	**(1.17)**	4.0919	**(-0.77)**
	SD	0.0100	**(-0.26)**	0.9678	**(1.17)**	4.0916	**(-0.78)**
L	**Pagano**	**0.0115**		**1.0368**		**3.8037**	
	HR3-RZT	0.0115	**(0.12)**	1.0461	**(0.90)**	3.7220	**(-2.15)**
	SD MCS	0.0115	**(0.15)**	1.0276	**(-0.89)**	3.8498	**(1.21)**
	SD	0.0115	**(0.15)**	1.0277	**(-0.88)**	3.8467	**(1.13)**
M	**Pagano**	**0.0226**		**1.4902**		**2.8969**	
	HR3-RZT	0.0225	**(-0.06)**	1.4908	**(0.04)**	2.9184	**(0.74)**
	SD MCS	0.0226	**(0.15)**	1.5172	**(1.81)**	2.9119	**(0.52)**
	SD	0.0226	**(0.02)**	1.5172	**(1.81)**	2.9120	**(0.52)**

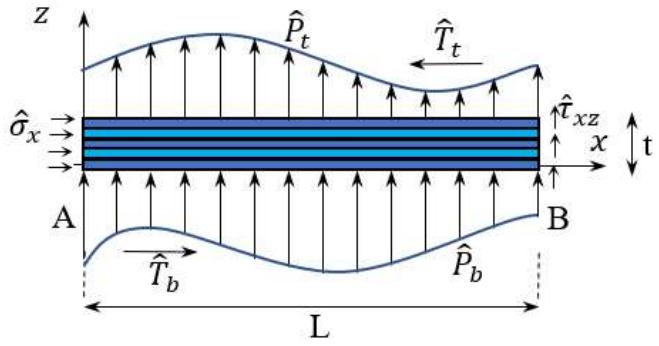

Fig. 1: Configuration of laminated beam with external tractions at top, bottom surfaces and beam ends A and B.

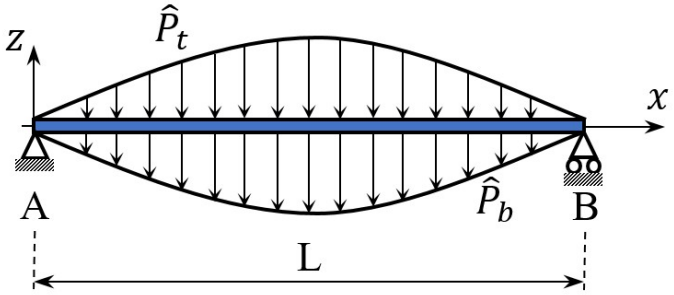

Fig. 2: Simply supported beam subject to a sinusoidal distributed load at top and bottom surfaces.

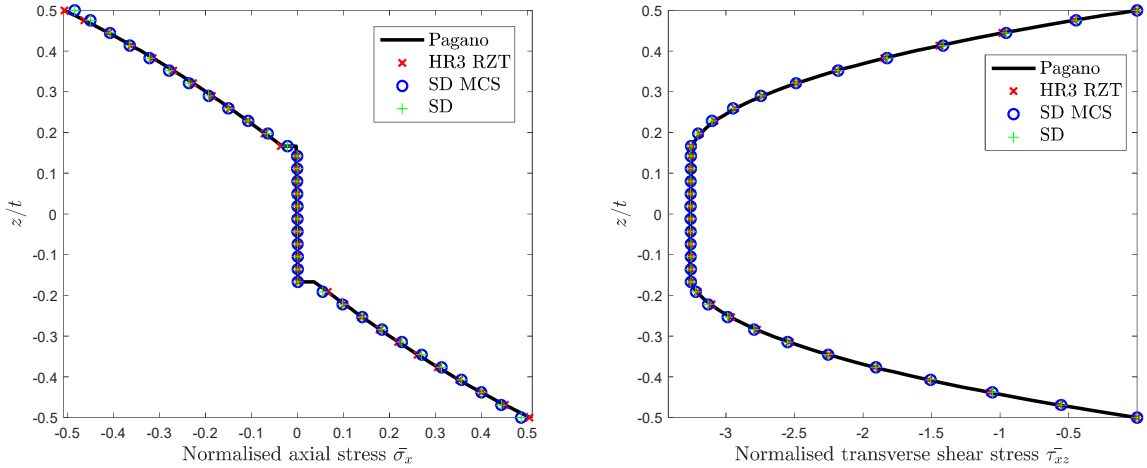

Fig. 3: Normalised axial stress and transverse shear stress for Laminate A.

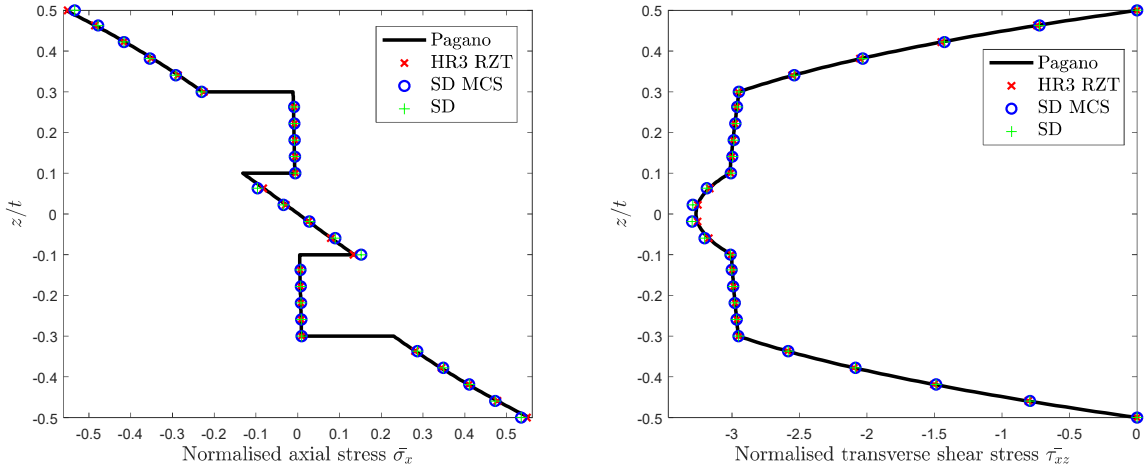

Fig. 4: Normalised axial stress and transverse shear stress for Laminate B.

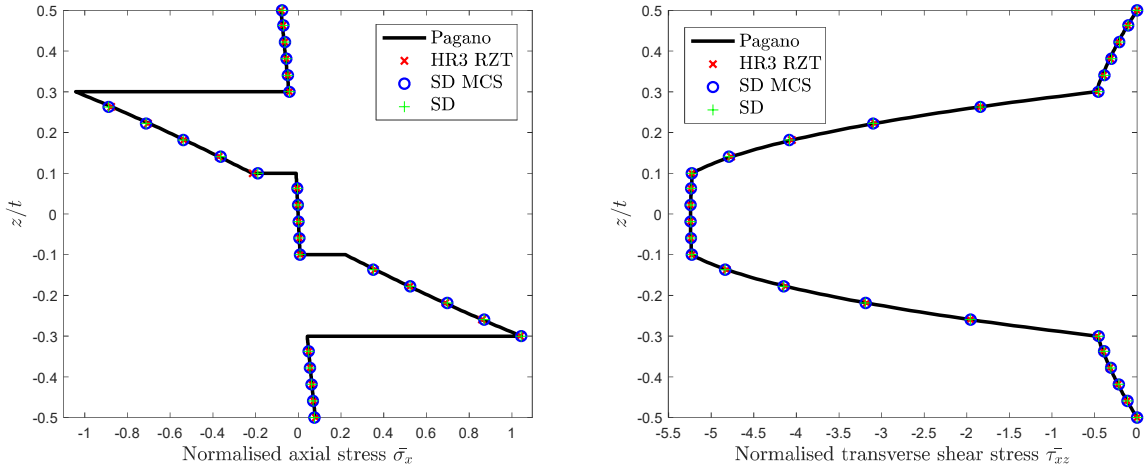

Fig. 5: Normalised axial stress and transverse shear stress for Laminate C.

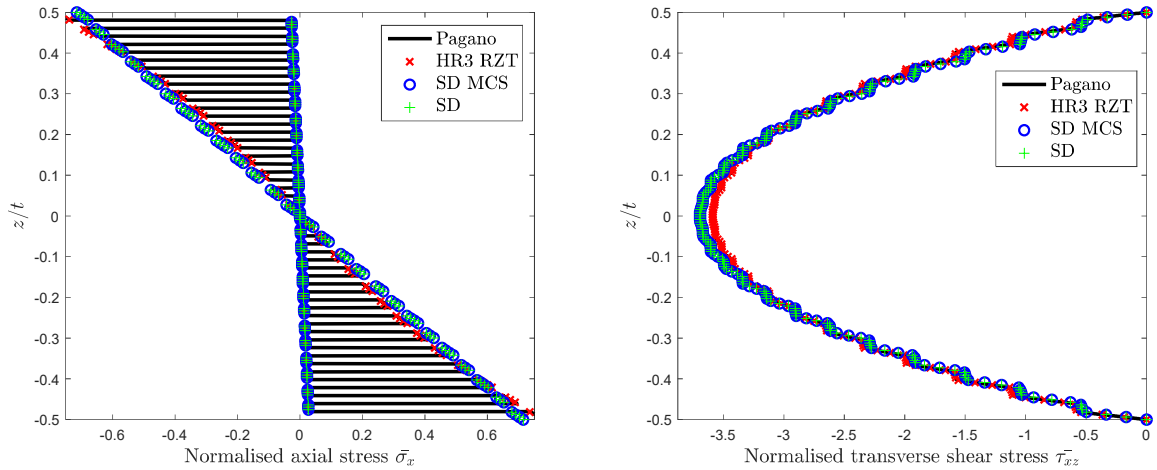

Fig. 6: Normalised axial stress and transverse shear stress for Laminate D.

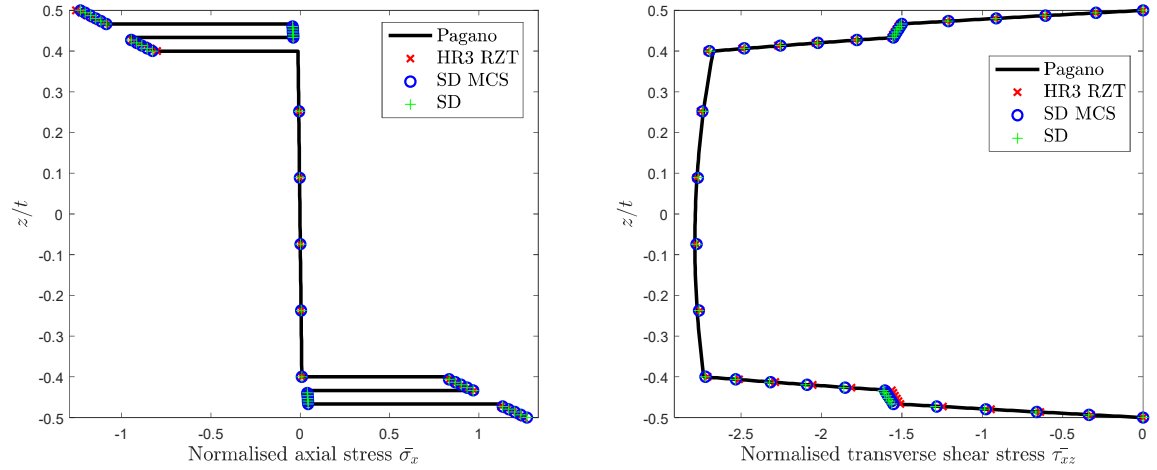

Fig. 7: Normalised axial stress and transverse shear stress for Laminate E.

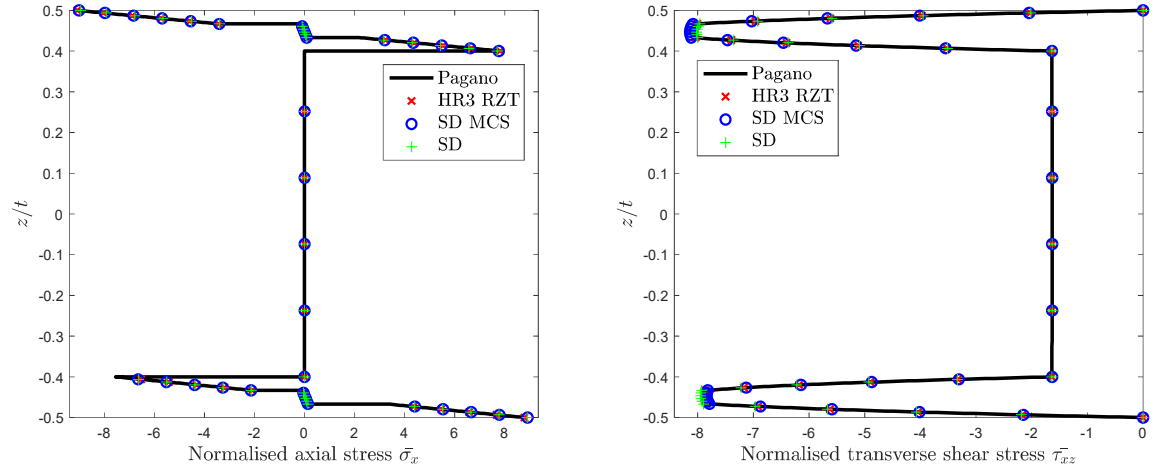

Fig. 8: Normalised axial stress and transverse shear stress for Laminate F.

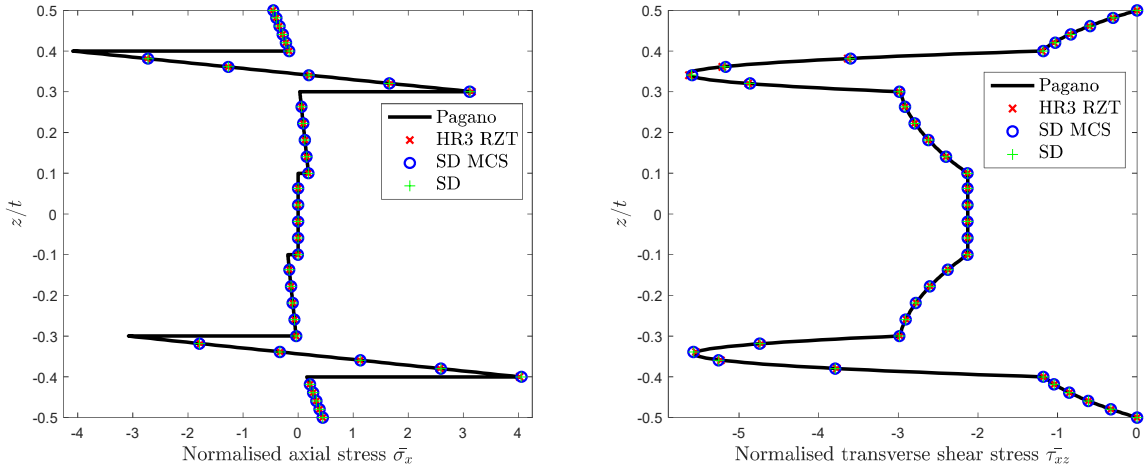

Fig. 9: Normalised axial stress and transverse shear stress for Laminate G.

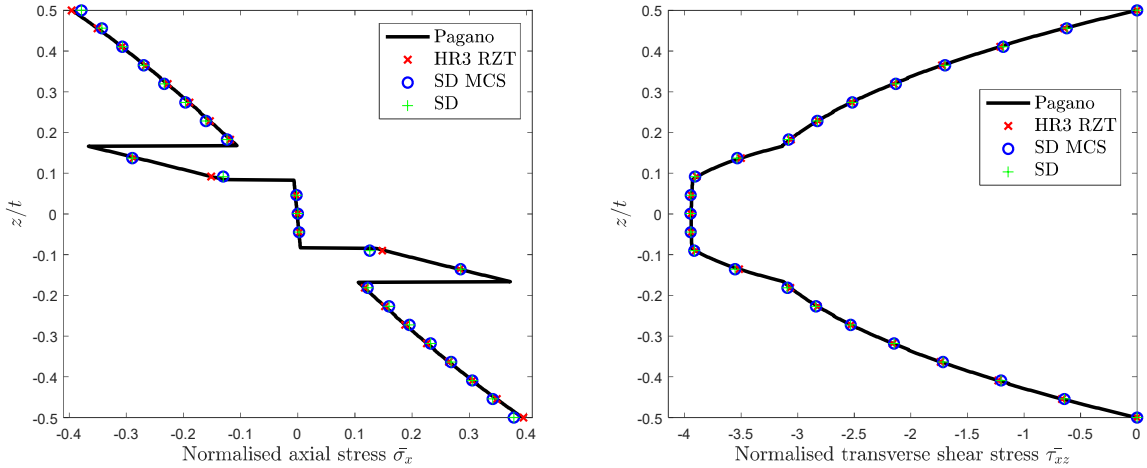

Fig. 10: Normalised axial stress and transverse shear stress for Laminate H.

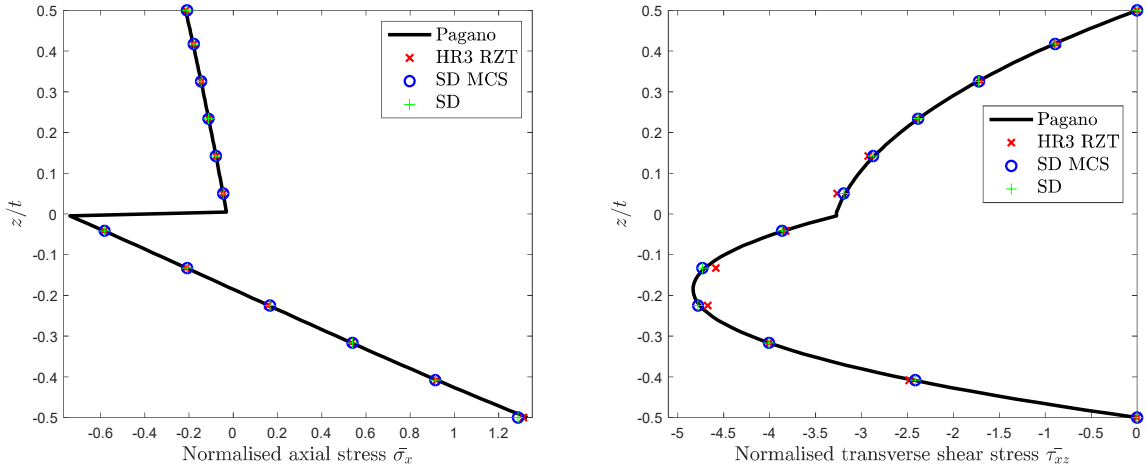

Fig. 11: Normalised axial stress and transverse shear stress for Laminate I.

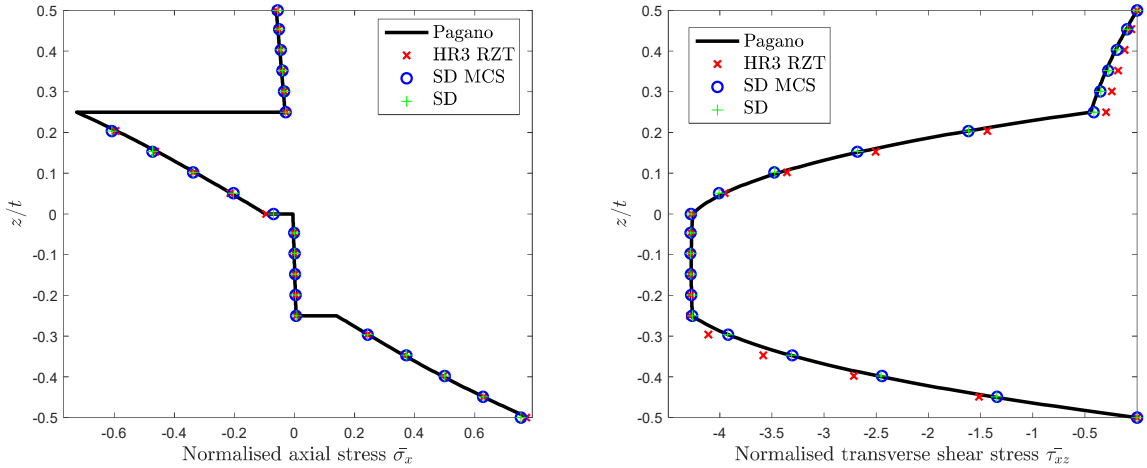

Fig. 12: Normalised axial stress and transverse shear stress for Laminate J.

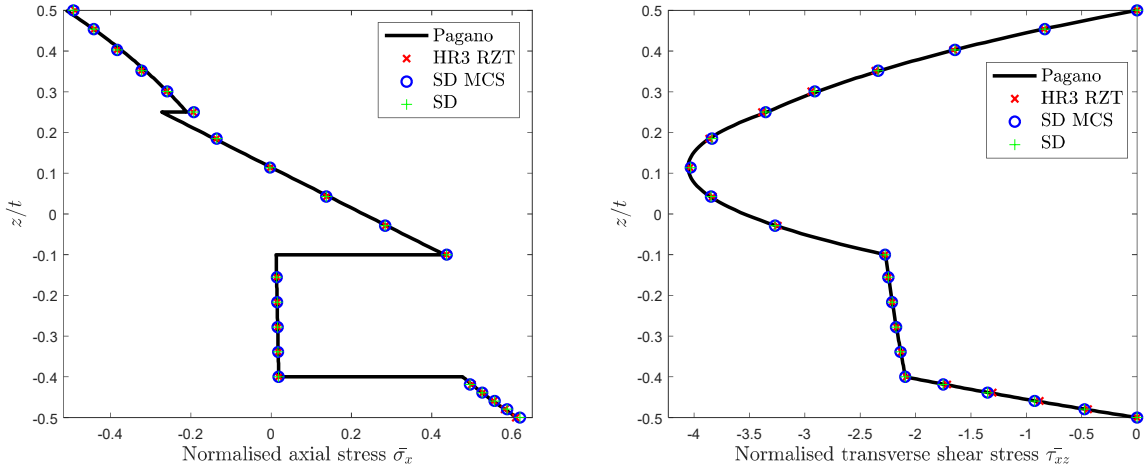

Fig. 13: Normalised axial stress and transverse shear stress for Laminate K.

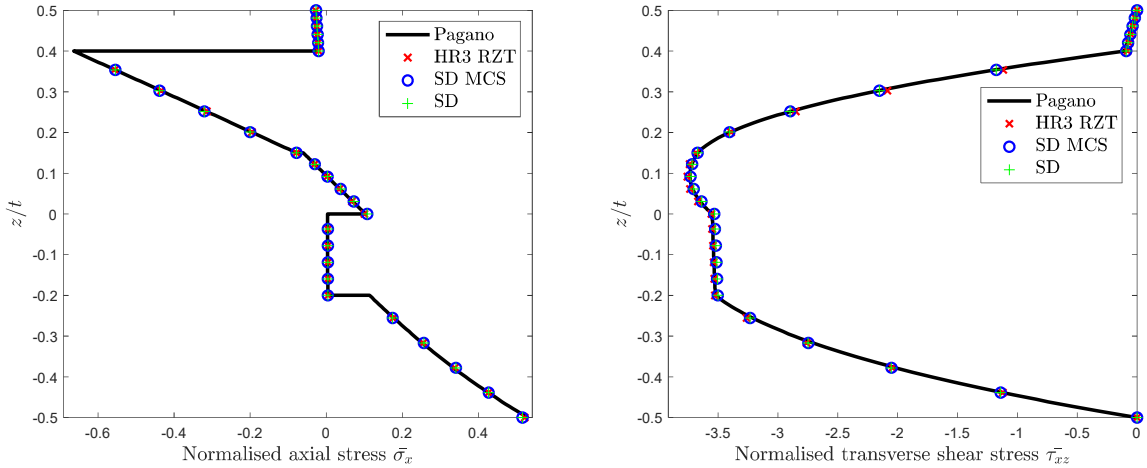

Fig. 14: Normalised axial stress and transverse shear stress for Laminate L.

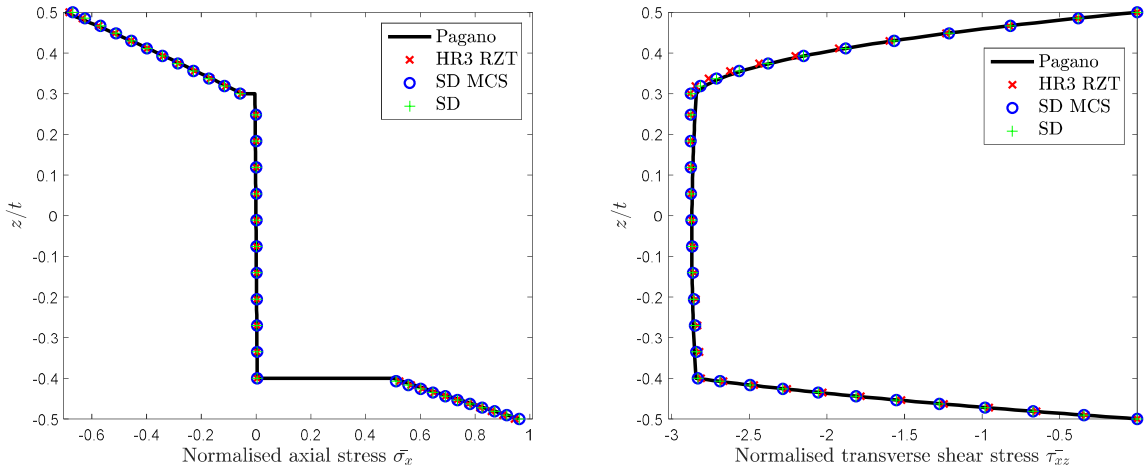

Fig. 15: Normalised axial stress and transverse shear stress for Laminate M.

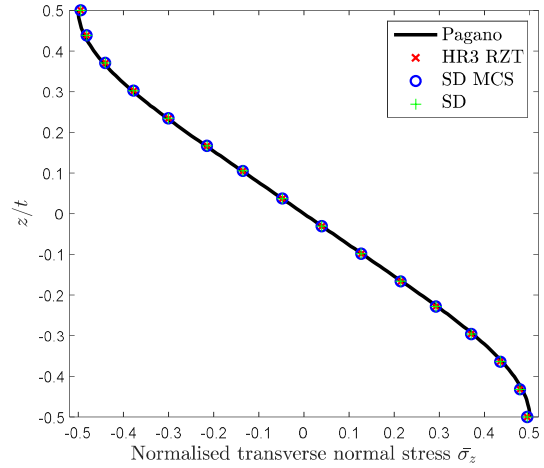

(a) Laminate A

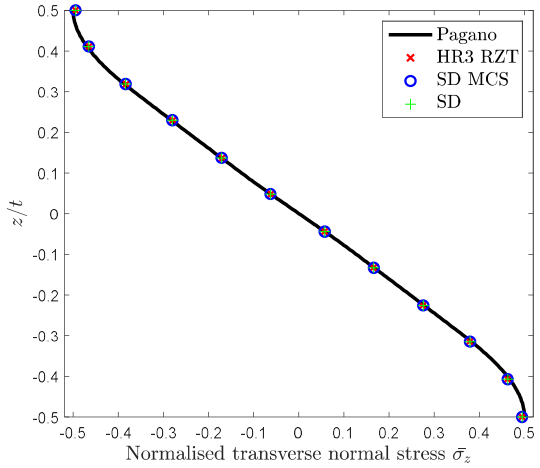

(b) Laminate B

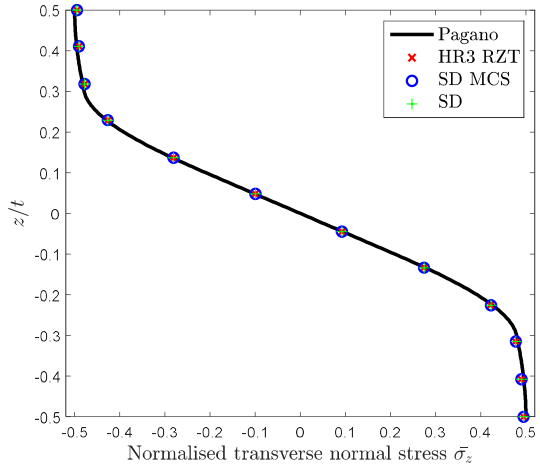

(c) Laminate C

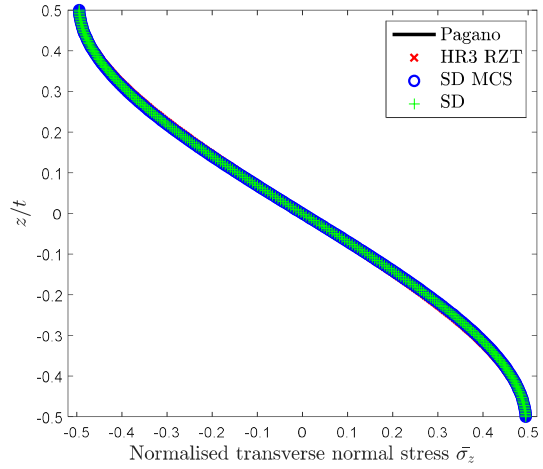

(d) Laminate D

Fig. 16: Normalised transverse normal stress for Laminates A-D.

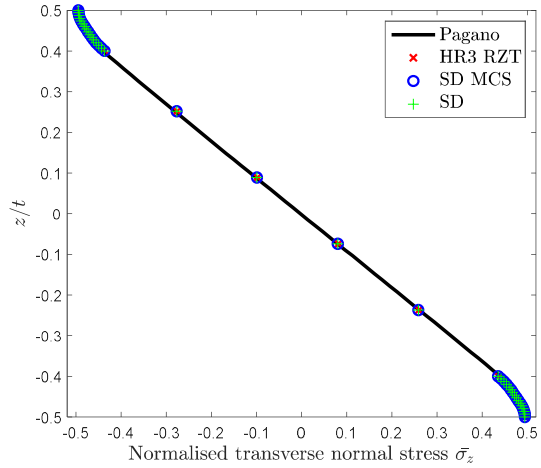

(a) Laminate E

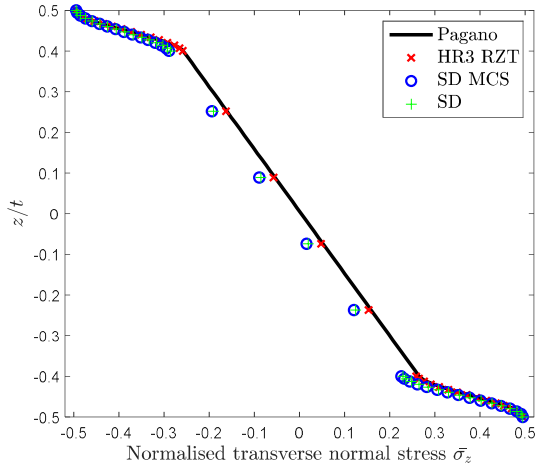

(b) Laminate F

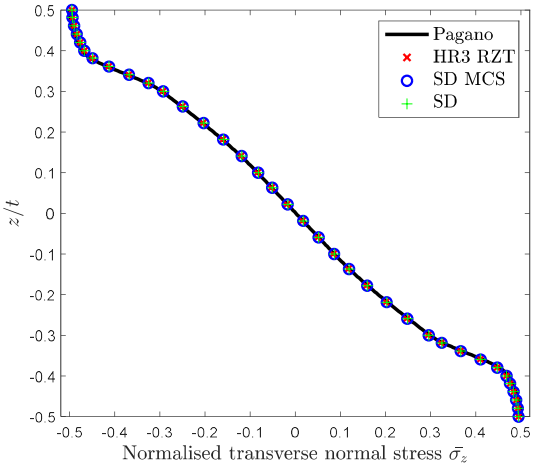

(c) Laminate G

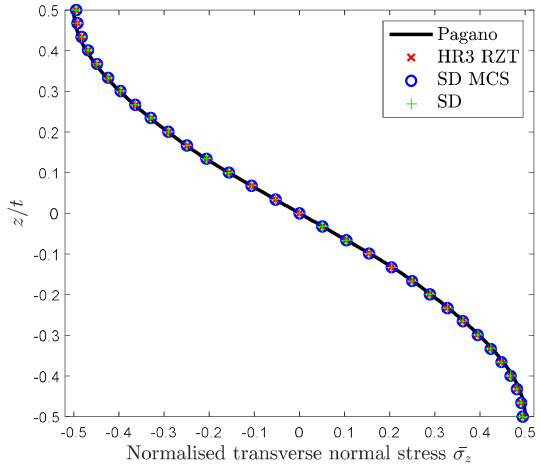

(d) Laminate H

Fig. 17: Normalised transverse normal stress for Laminates E-H.

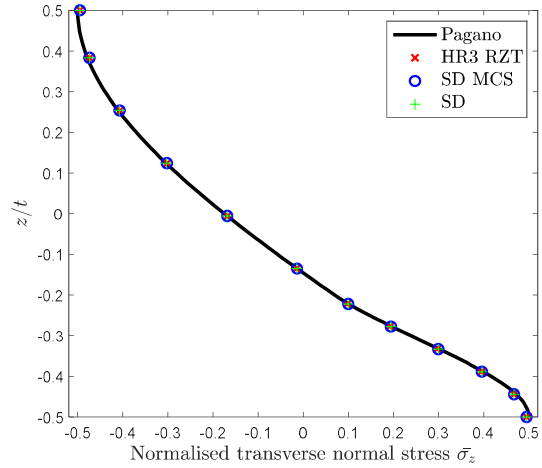

(a) Laminate I

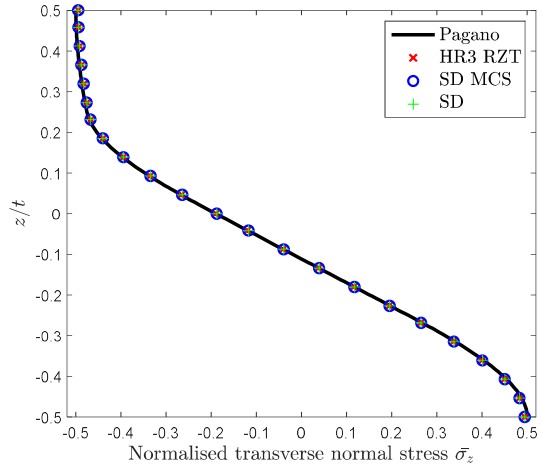

(b) Laminate J

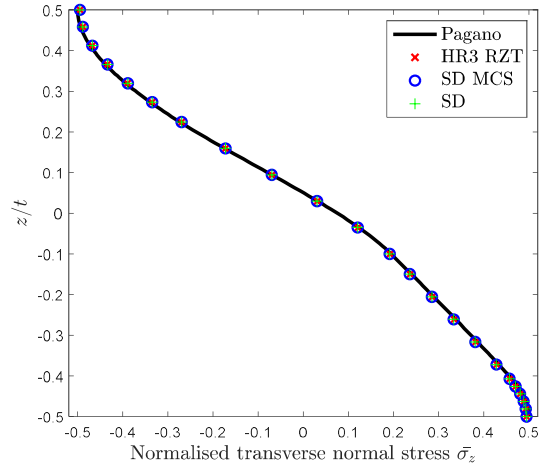

(c) Laminate K

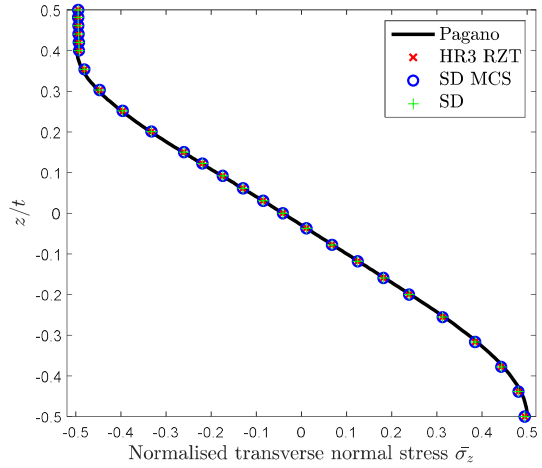

(d) Laminate L

Fig. 18: Normalised transverse normal stress for Laminates I-L.

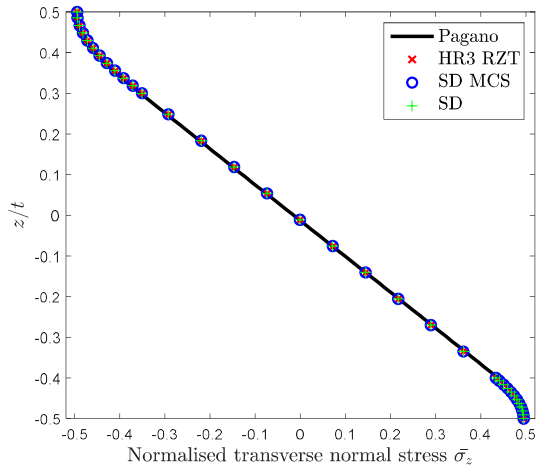

Fig. 19: Normalised transverse normal stress for Laminate M.

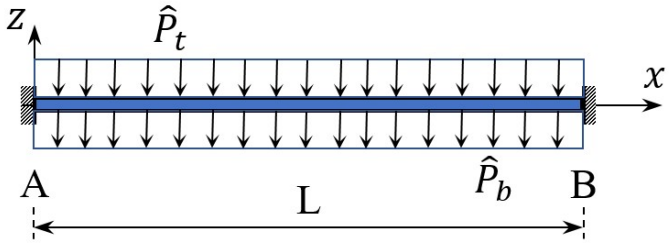

Fig. 20: Clamped beam subject to a uniform distributed load at top and bottom surfaces.

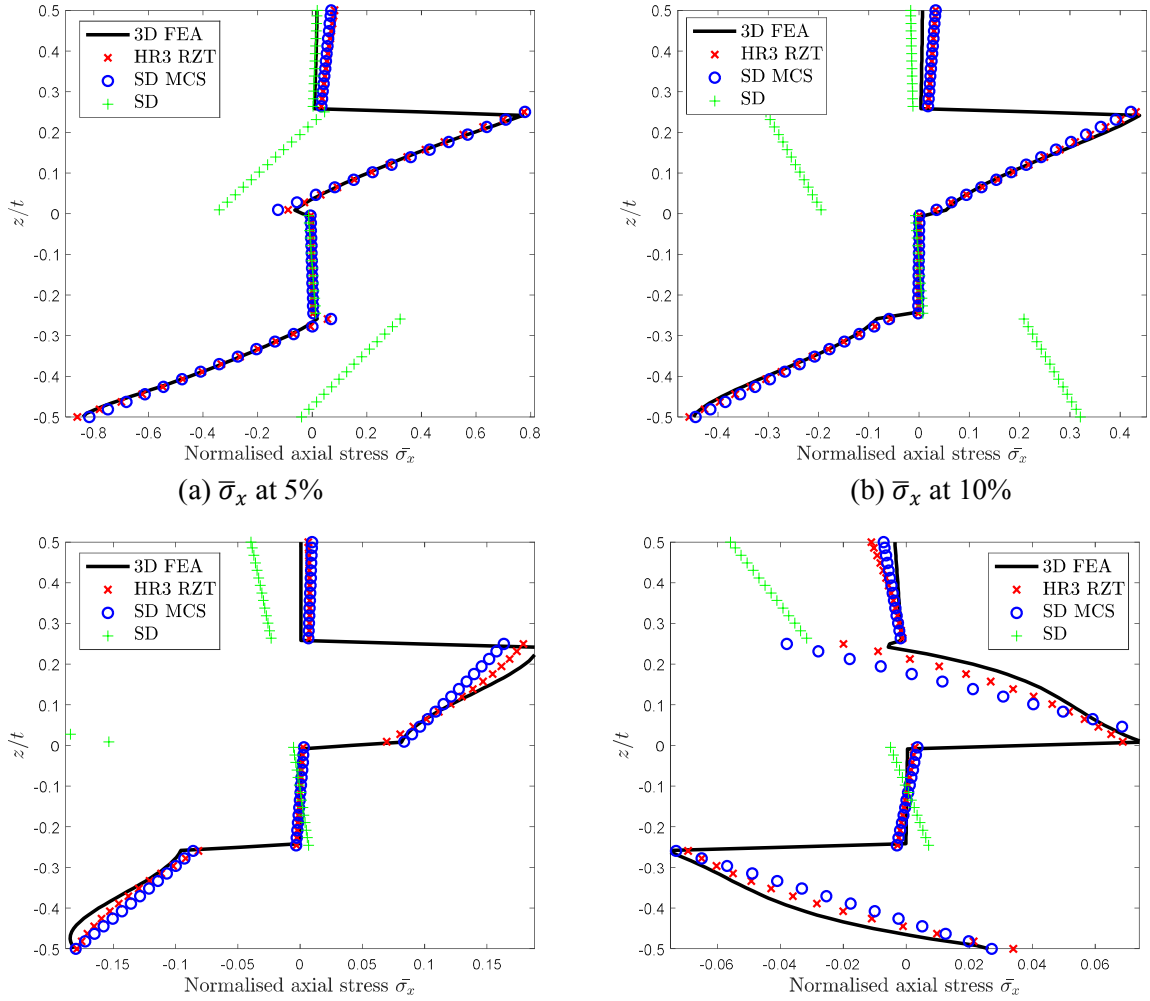

(a) $\overline{\sigma}_x$ at 5%

(b) $\overline{\sigma}_x$ at 10%

(c) $\overline{\sigma}_x$ at 15%

(d) $\overline{\sigma}_x$ at 20%

Fig. 21: Normalised axial stress at the locations 5%, 10%, 15% and 20% of span from the clamped end A.

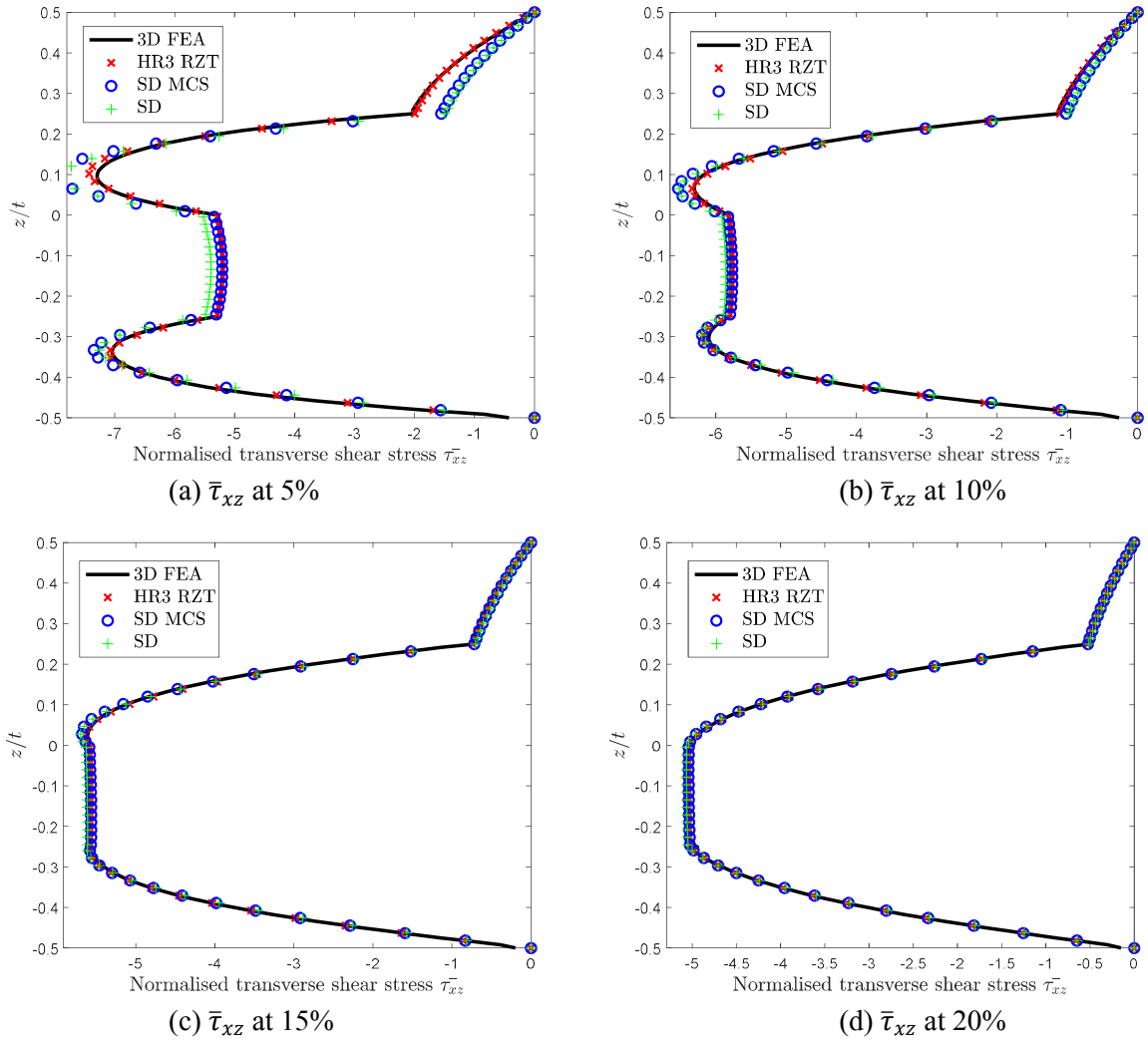

(a) $\bar{\tau}_{xz}$ at 5%

(b) $\bar{\tau}_{xz}$ at 10%

(c) $\bar{\tau}_{xz}$ at 15%

(d) $\bar{\tau}_{xz}$ at 20%

Fig. 22: Normalised shear stress at the locations 5%, 10%, 15% and 20% of span from the clamped end A.

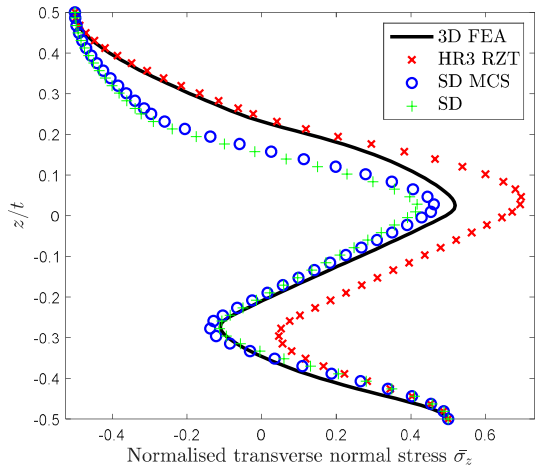

(a) $\overline{\sigma}_z$ at 5%

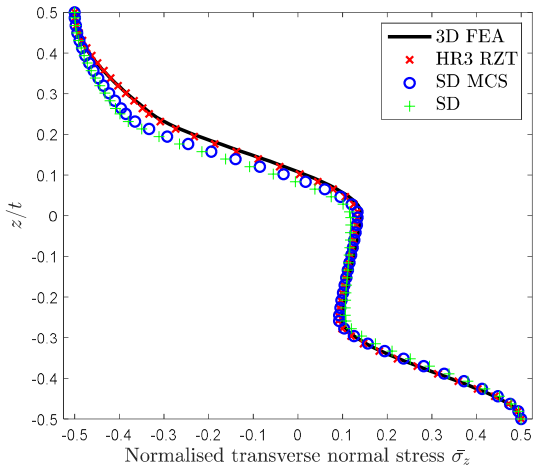

(b) $\overline{\sigma}_z$ at 10%

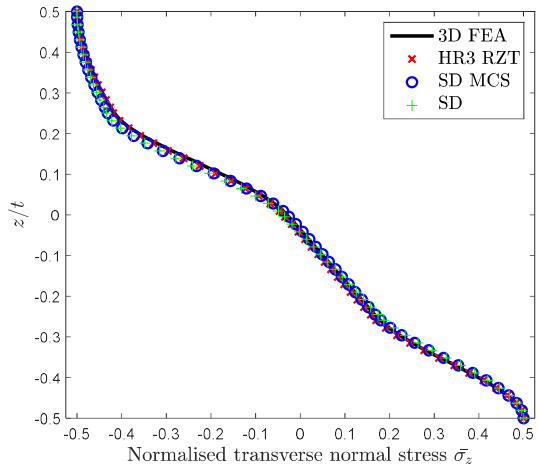

(c) $\overline{\sigma}_z$ at 15%

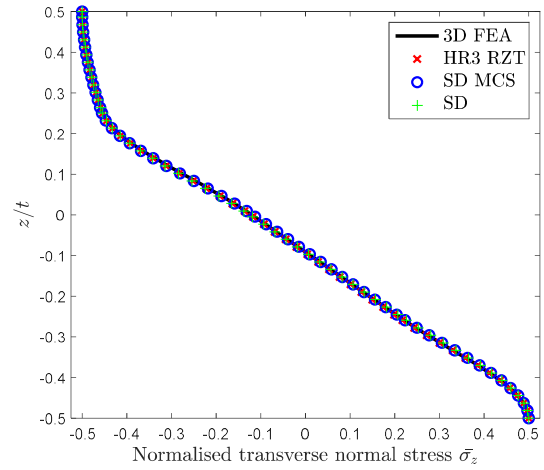

(d) $\overline{\sigma}_z$ at 20%

Fig. 23: Normalised transverse normal stress at the locations 5%, 10%, 15% and 20% of span from the clamped end A.

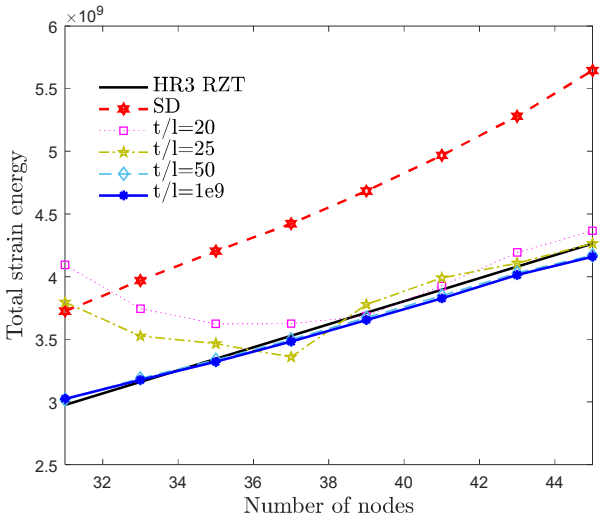

Fig. 24: Strain energy with respect to different length scales in the constitutive relation of couple stress.

[1] Jones R. Mechanics of composite materials. London, UK: Taylor & Francis Ltd.; 1998.
[2] Timoshenko S, Goodier J. Theory of elasticity. New York: McGraw-Hill; 1970.
[3] Whitney JM, Pagano NJ. Shear deformation in heterogeneous anisotropic plates. Journal of Applied Mechanics. 1970;37:1031–6.
[4] Polizzotto C. From the Euler–Bernoulli beam to the Timoshenko one through a sequence of Reddy-type shear deformable beam models of increasing order. European Journal of Mechanics - A/Solids. 2015;53:62-74.
[5] Groh RMJ, Tessler A. Computationally efficient beam elements for accurate stresses in sandwich laminates and laminated composites with delaminations. Computer Methods in Applied Mechanics and Engineering. 2017;320:369-95.
[6] Groh RMJ, Weaver PM, Tessler A. Application of the Refined Zigzag Theory to the Modeling of Delaminations in Laminated Composites. NASA/TM-2015-218808; 2015.
[7] Tessler A. Refined zigzag theory for homogeneous, laminated composite, and sandwich beams derived from Reissner's mixed variational principle. Meccanica. 2015;50(10):2621-48.
[8] Tessler A. An improved plate theory of {1,2}-order for thick composite laminates. International Journal of Solids and Structures. 1993;30(7):981-1000.
[9] Tessler A, Sciuva MD, Gherlone M. Refinement of Timoshenko beam theory for composite and sandwich beams using zigzag kinematics. NASA/TP-2007-2150862007.
[10] Filippi M, Carrera E. Bending and vibrations analyses of laminated beams by using a zig-zag-layer-wise theory. Composites Part B: Engineering. 2016;98:269-80.
[11] Filippi M, Carrera E, Valvano S. Analysis of multilayered structures embedding viscoelastic layers by higher-order, and zig-zag plate elements. Composites Part B: Engineering. 2018;154:77-89.
[12] Filippi M, Pagani A, Petrolo M, Colonna G, Carrera E. Static and free vibration analysis of laminated beams by refined theory based on Chebyshev polynomials. Composite Structures. 2015;132:1248-59.
[13] Vo TP, Nguyen T-K, Thai H-T, Lanc D, Karamanli A. Flexural analysis of laminated composite and sandwich beams using a four-unknown shear and normal deformation theory. Composite Structures. 2017;176:388–97.
[14] Vo TP, Thai H-T. Static behavior of composite beams using various refined shear deformation theories. Composite Structures. 2012;94:2513–22.
[15] Di Capua D, Oñate E. Two-noded zigzag beam element accounting for shear effects based on an extended Euler Bernoulli theory. Composite Structures. 2015;132:1192-205.
[16] Oñate E, Eijo A, Oller S. Simple and accurate two-noded beam element for composite laminated beams using a refined zigzag theory. Computer Methods in Applied Mechanics and Engineering. 2012;213-216:362-82.
[17] Chai GB, Yap CW. Coupling effects in bending, buckling and free vibration of generally laminated composite beams. Composites Science and Technology. 2008;68(7-8):1664-70.
[18] Banerjee JR, Ananthapuvirajah A. An exact dynamic stiffness matrix for a beam incorporating Rayleigh–Love and Timoshenko theories. International Journal of Mechanical Sciences. 2019;150:337-47.
[19] Shi W, Shen ZB, Peng XL, Li XF. Frequency equation and resonant frequencies of free–free Timoshenko beams with unequal end masses. International Journal of Mechanical Sciences. 2016;115-116:406-15.
[20] Alashti RA, Abolghasemi AH. A Size-dependent Bernoulli-Euler Beam Formulation based on a New Model of Couple Stress Theory. International Journal of Engineering. 2014;27(6 (C)).
[21] Mohammad Abadi M, Daneshmehr AR. An investigation of modified couple stress theory in buckling analysis of micro composite laminated Euler–Bernoulli and Timoshenko beams. International Journal of Engineering Science. 2014;75:40-53.
[22] Chen WJ, Li XP. Size-dependent free vibration analysis of composite laminated Timoshenko beam based on new modified couple stress theory. Archive of Applied Mechanics. 2012;83(3):431-44.
[23] Dehrouyeh-Semnani AM, Bahrami A. On size-dependent Timoshenko beam element based on modified couple stress theory. International Journal of Engineering Science. 2016;107:134-48.
[24] Romanoff J, Reddy JN. Experimental validation of the modified couple stress Timoshenko beam theory for web-core sandwich panels. Composite Structures. 2014;111:130-7.
[25] Roque CMC, Fidalgo DS, Ferreira AJM, Reddy JN. A study of a microstructure-dependent composite laminated Timoshenko beam using a modified couple stress theory and a meshless method. Composite Structures. 2013;96:532-7.
[26] Carrera E, Giunta G, Petrolo M. Beam structures: classical and advanced theories: John Wiley & Sons; 2011.
[27] Minera S, Patni M, Carrera E, Petrolo M, Weaver PM, Pirrera A. Three-dimensional stress analysis for beam-like structures using Serendipity Lagrange shape functions. International Journal of Solids and Structures. 2018.
[28] Pagani A, de Miguel AG, Carrera E. Cross-sectional mapping for refined beam elements with applications to shell-like structures. Computational Mechanics. 2017;59(6):1031-48.
[29] Pagani A, Yan Y, Carrera E. Exact solutions for static analysis of laminated, box and sandwich beams by refined layer-wise theory. Composites Part B: Engineering. 2017;131:62-75.
[30] Wu B, Pagani A, Filippi M, Chen WQ, Carrera E. Accurate stress fields of post-buckled laminated composite beams accounting for various kinematics. International Journal of Non-Linear Mechanics. 2019;111:60-71.

[31] Yan Y, Carrera E, de Miguel AG, Pagani A, Ren QW. Meshless analysis of metallic and composite beam structures by advanced hierarchical models with layer-wise capabilities. Composite Structures. 2018;200:380-95.
[32] Zappino E, Viglietti A, Carrera E. Analysis of tapered composite structures using a refined beam theory. Composite Structures. 2018;183:42-52.
[33] Zappino E, Viglietti A, Carrera E. The analysis of tapered structures using a component-wise approach based on refined one-dimensional models. Aerospace Science and Technology. 2017;65:141-56.
[34] Vo TP, Thai H-T, Inam F. Axial-flexural coupled vibration and buckling of composite beams using sinusoidal shear deformation theory. Archive of Applied Mechanics. 2012;83(4):605-22.
[35] Ferreira AJM, Carrera E, Cinefra M, Viola E, Tornabene F, Fantuzzi N, et al. Analysis of thick isotropic and cross-ply laminated plates by generalized differential quadrature method and a Unified Formulation. Composites Part B: Engineering. 2014;58:544-52.
[36] Zenkour AM. Transverse shear and normal deformation theory for bending analysis of laminated and sandwich elastic beams. Mechanics of Composite Materials and Structures. 1999;6(3):267-83.
[37] Mantari JL, Canales FG. Finite element formulation of laminated beams with capability to model the thickness expansion. Composites Part B: Engineering. 2016;101:107-15.
[38] Mantari JL, Oktem AS, Guedes Soares C. A new higher order shear deformation theory for sandwich and composite laminated plates. Composites Part B: Engineering. 2012;43:1489–99.
[39] Carrera E. Historical review of Zig-Zag theories for multilayered plates and shells. Applied Mechanics Reviews. 2003;56(3):287-308.
[40] Tessler A, Sciuva MD, Gherlone M. Refined Zigzag Theory for Laminated Composite and Sandwich Plates. National Aeronautics and Space Administration. Washington, D.C.,2009.
[41] Groh RMJ, Weaver PM. On displacement-based and mixed-variational equivalent single layer theories for modelling highly heterogeneous laminated beams. International Journal of Solids and Structures. 2015;59:147-70.
[42] Barut A, Madenci E, Tessler A. A Refined Zigzag Theory for Laminated Composite and Sandwich Plates Incorporating Thickness Stretch Deformation. 2012.
[43] Barut A, Madenci E, Tessler A. C0-continuous triangular plate element for laminated composite and sandwich plates using the {2,2} – Refined Zigzag Theory. Composite Structures. 2013;106:835-53.
[44] Di Sciuva M, Sorrenti M. Bending and free vibration analysis of functionally graded sandwich plates: An assessment of the Refined Zigzag Theory. Journal of Sandwich Structures & Materials. 2019.
[45] Fares ME, Elmarghany MK. A refined zigzag nonlinear first-order shear deformation theory of composite laminated plates. Composite Structures. 2008;82(1):71-83.
[46] Flores FG, Oller S, Nallim LG. On the analysis of non-homogeneous laminates using the refined zigzag theory. Composite Structures. 2018;204:791-802.
[47] Iurlaro L, Gherlone M, Di Sciuva M. The (3,2)-Mixed Refined Zigzag Theory for generally laminated beams: Theoretical development and C0 finite element formulation. International Journal of Solids and Structures. 2015;73-74:1-19.
[48] Iurlaro L, Gherlone M, Di Sciuva M, Tessler A. Refined Zigzag Theory for laminated composite and sandwich plates derived from Reissner's Mixed Variational Theorem. Composite Structures. 2015;133:809-17.
[49] Nallim LG, Oller S, Oñate E, Flores FG. A hierarchical finite element for composite laminated beams using a refined zigzag theory. Composite Structures. 2017;163:168-84.
[50] Versino D, Gherlone M, Di Sciuva M. Four-node shell element for doubly curved multilayered composites based on the Refined Zigzag Theory. Composite Structures. 2014;118:392-402.
[51] Eringen AC. Theory of Micropolar Elasticity. Defense Technical Information Center; 1967.
[52] Eringen AC. Linear theory of micropolar elasticity. Journal of Mathematics and Mechanics. 1966;15(6):909-23.
[53] Eringen AC. Microcontinuum field theories I: Foundation and solids. Newyork: Springer Science+Business Media, LLC; 1999.
[54] Eringen AC. Microcontinuum field theories: II. Fuent Media. Newyork: Springer-Verlag; 2001.
[55] Mindlin RD. Influence of couple-stresses on stress concentrations. Experimental Mechanics. 1962;3(1):1-7.
[56] Mindlin RD. Micro-structure in linear elasticity. Archives of Rational Mechanics and Analysis. 1964;16:51-78.
[57] Mindlin RD, Eshel NN. On first strain-gradient theories in linear elasticity. International journal of solids structures. 1968;4:109-24.
[58] Mindlin RD, Tiersten HF. Effects of Couple-stressesin Linear Elasticity. Archive for Rational Mechanics and Analysis. 1962;11(1):415–48.
[59] Yang F, Chong ACM, Lam DCC, Tong P. Couple stress based strain gradient theory for elasticity. International Journal of Solids and Structures. 2002;39:2731–43.
[60] Lam DCC, Yang F, Chong ACM, Wang J, Tong P. Experiments and theory in strain gradient elasticity. Journal of the Mechanics and Physics of Solids. 2003;51(8):1477-508.
[61] Chen W, Li L, Xu M. A modified couple stress model for bending analysis of composite laminated beams with first order shear deformation. Composite Structures. 2011;93(11):2723-32.
[62] Chen W, Xu M, Li L. A model of composite laminated Reddy plate based on new modified couple stress theory. Composite Structures. 2012;94(7):2143-56.
[63] Washizu K. Variational Methods in Elasticity and Plasticity , 2ed. London, UK: Pergamon press; 1975.

[64] Stolarski H, Belytschko T. On the equivalence of mode decomposition and mixed finite elements based on the Hellinger-Reissner principle. part I: Theory. Computer Methods in Applied Mechanics and Engineering. 1986;58:249 –63.
[65] Reissner E. On a certain mixed variational theorem and a proposed application. International Journal for Numerical Methods in Engineering. 1984;20(7):1366 –8.
[66] Militello C, Felippa CA. A variational natural justification strain formulation finite elements. NASA-CR-189063; 1991.
[67] Auricchio F, Balduzzi G, Khoshgoftar MJ, Rahimi G, Sacco E. Enhanced modeling approach for multilayer anisotropic plates based on dimension reduction method and Hellinger–Reissner principle. Composite Structures. 2014;118:622-33.
[68] Auricchio F, Balduzzi G, Lovadina C. The dimensional reduction modelling approach for 3D beams: Differential equations and finite-element solutions based on Hellinger–Reissner principle. International Journal of Solids and Structures. 2013;50(25-26):4184-96.
[69] Auricchio F, Balduzzi G, Lovadina C. The dimensional reduction approach for 2D non-prismatic beam modelling: A solution based on Hellinger–Reissner principle. International Journal of Solids and Structures. 2015;63:264-76.
[70] Beltempo A, Balduzzi G, Alfano G, Auricchio F. Analytical derivation of a general 2D non-prismatic beam model based on the Hellinger–Reissner principle. Engineering Structures. 2015;101:88-98.
[71] Viebahn N, Steeger K, Schröder J. A simple and efficient Hellinger–Reissner type mixed finite element for nearly incompressible elasticity. Computer Methods in Applied Mechanics and Engineering. 2018;340:278-95.
[72] Cosentino E, Weaver PM. An enhanced single-layer variational formulation for the effect of transverse shear on laminated orthotropic plates. European Journal of Mechanics - A/Solids. 2010;29(4):567-90.
[73] Kwon Y-R, Lee B-C. A mixed element based on Lagrange multiplier method for modified couple stress theory. Computational Mechanics. 2016;59(1):117-28.
[74] Zenkour AM. A novel mixed nonlocal elasticity theory for thermoelastic vibration of nanoplates. Composite Structures. 2018;185:821-33.
[75] Groh RMJ. Non-classical effects in straight-fibre and towsteered composite beams and plates. Doctoral thesis: University of Bristol; 2015.
[76] Kwon Y-R, Lee B-C. Three dimensional elements with Lagrange multipliers for the modified couple stress theory. Computational Mechanics. 2017;62(1):97-110.
[77] Nguyen N-D, Nguyen T-K, Thai H-T, Vo TP. A Ritz type solution with exponential trial functions for laminated composite beams based on the modified couple stress theory. Composite Structures. 2018;191:154-67.
[78] Yang W, He D, Chen W. A size-dependent zigzag model for composite laminated micro beams based on a modified couple stress theory. Composite Structures. 2017;179:646-54.
[79] Pagano NJ. Exact solutions for composite laminates in cylindrical bending. Journal of composite materials. 1969;3:398-411.
[80] Gherlone M. On the Use of Zigzag Functions in Equivalent Single Layer Theories for Laminated Composite and Sandwich Beams: A Comparative Study and Some Observations on External Weak Layers. Journal of Applied Mechanics. 2013;80(6):1-19.
[81] Patni M, Minera S, Groh RMJ, Pirrera A, Weaver PM. Three-dimensional stress analysis for laminated composite and sandwich structures. Composites Part B: Engineering. 2018;155:299-328.
[82] Trinh LC. Behaviours of functionally graded sandwich micro-beams and plates. Doctoral thesis: Northumbria University; 2017.
[83] Nguyen HX. Isogeometric Analysis of Small-Scale Plates with Generalised Continua. Doctoral thesis: Northumbria University; 2018.